U.S. DEPARTMENT OF THE INTERIOR
U.S. GEOLOGICAL SURVEY

AEROMAGNETIC AND GRAVITY MAPS OF THE CENTRAL MARYSVALE VOLCANIC FIELD, SOUTHWESTERN UTAH

By

David L. Campbell, Thomas A. Steven, Charles G. Cunningham, and Peter D. Rowley

Pamphlet to accompany
GEOLOGIC INVESTIGATIONS SERIES I–2645–B

The photograph on the cover of the map jacket shows a view looking west-southwest into the Mount Belknap caldera from a point on its eastern topographic wall. Mount Belknap (elev. 12,139 ft) is the peak on the right. The smooth slopes and cliffs reflect the eruptive sequence of ash flow tuffs and cliff-forming rhyolite lava flows.

CONTENTS

FIGURES

TABLES

AEROMAGNETIC AND GRAVITY MAPS OF THE CENTRAL MARYSVALE VOLCANIC FIELD, SOUTHWESTERN UTAH

By
David L. Campbell, Thomas A. Steven,
Charles G. Cunningham, and Peter D. Rowley

ABSTRACT

Gravity and aeromagnetic features in the Marysvale volcanic field result from the composite effects of many factors, including rock composition, style of magmatic emplacement, type and intensity of rock alteration, and effects of structural evolution.

Densities and magnetic properties measured on a suite of rock samples from the Marysvale volcanic field differ in systematic ways. Generally, the measured densities, magnetic susceptibilities, and natural remanent magnetizations all increase with mafic index, but decrease with degree of alteration, and for tuffs, with degree of welding. Koenigsberger Q indices show no such systematic trends.

The study area is divided into three geophysical domains. The northern domain is dominated by aeromagnetic lows that probably reflect reversed-polarity volcanic flows. There are no intermediate-sized magnetic highs in the northern domain that might reflect plutons. The northern domain has a decreasing-to-the-south gravity gradient that reflects the Pavant Range homocline. The central domain has gravity lows that reflect altered rocks in calderas and low-density plutons of the Marysvale volcanic field. Its aeromagnetic signatures consist of rounded highs that reflect plutons and birdseye patterns that reflect volcanic flows. In many places the birdseyes are attenuated, indicating that the flows there have been hydrothermally altered. We interpret the central domain to reflect an east-trending locus of plutons in the Marysvale volcanic field. The southern domain has intermediate gravity fields, indicating somewhat denser rocks there than in the central domain, and high-amplitude aeromagnetic birdseyes that reflect unaltered volcanic units. The southern domain contains no magnetic signatures that we interpret to reflect plutons.

Basin-and-range tectonism has overprinted additional gravity features on the three domains. A deep gravity low follows the Sevier and Marysvale Valleys, reflecting grabens there. The gravity gradient in the north reflects the southern flank of a structural dome that led to the Pavant Range homocline and whose southern edge lies along the Clear Creek downwarp.

INTRODUCTION AND PREVIOUS WORK

The Marysvale volcanic field of southwestern Utah is located at the eastern end of the broad belt of Tertiary igneous rocks (Pioche-Marysvale igneous belt) that extends east-northeast from southern Nevada to central Utah (fig. l). The volcanic field is situated largely in the High Plateaus subprovince which marks the transition between the Colorado Plateau and the Basin and Range provinces and is one of several volcanic fields that surround the Colorado Plateau. A long history of mining in the Tushar Mountains and adjoining areas for gold, silver, lead, zinc, uranium, iron, and industrial minerals has attracted sporadic geologic study since the late l800's. In l975 T.A. Steven and C.G. Cunningham of the U.S. Geological Survey began remapping the Tushar Mountains and adjacent areas, and these studies evolved into a regional multidisciplinary investigation of the mineral resource potential of the Richfield $1^\circ \times 2^\circ$ quadrangle under the U. S. Geological Survey's Conterminous United States Mineral Appraisal Program (CUSMAP). Major CUSMAP publications about the Marysvale volcanic field include colored geologic maps at scales of l:250,000 and 1:500,000 (Steven and others, l990), l:50,000 (Cunningham and others, l983; Steven and Morris, l986), l:24,000 (Rowley and others,1986a,b, l988a,b), gravity maps at various scales (Cook and others, l980, l98l, l984; Halliday and Cook, l980), aeromagnetic maps (Campbell and others, l984), volcanological studies (Budding and others, l987; Cunningham and Steven, l979a; Rowley and others, l979, 1981; Steven

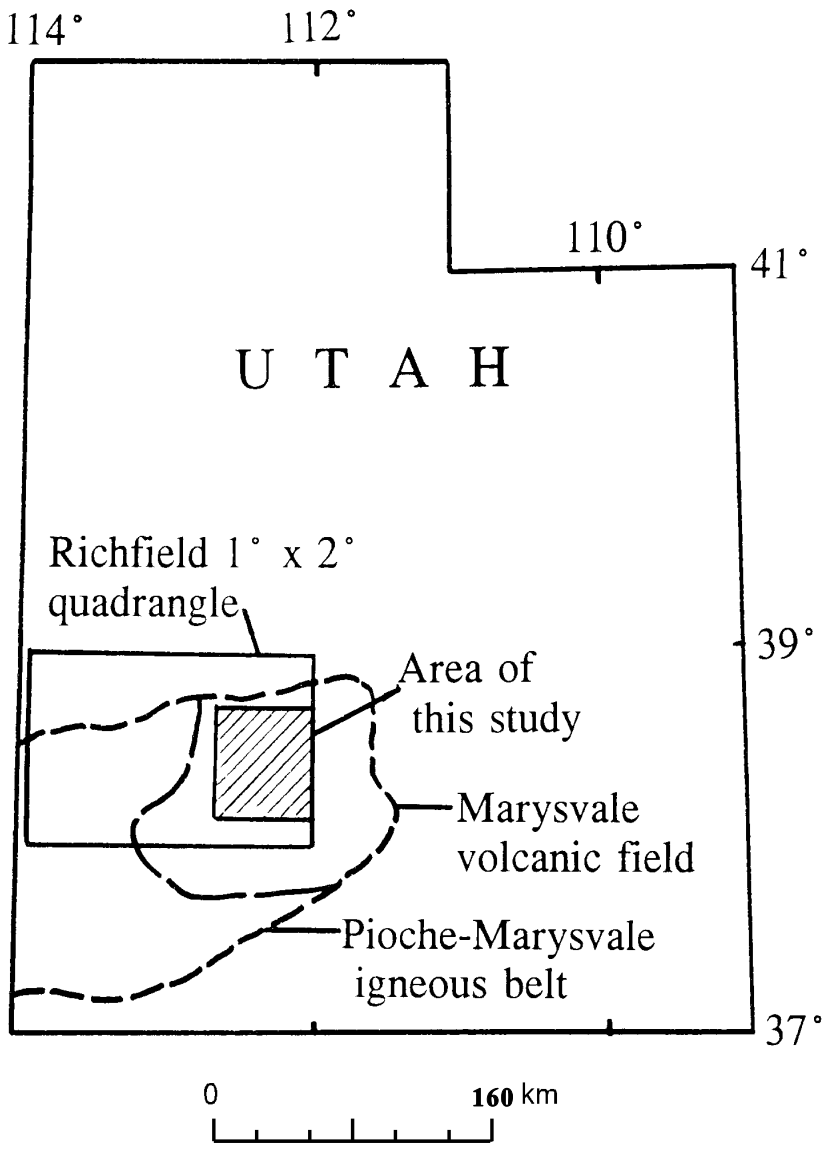

Figure 1. Index map of Utah showing location of the Pioche-Marysvale igneous belt in southwestern Utah, the Marysvale volcanic field, area of the Richfield 1°× 2° quadrangle, and area of this study (Tushar Mountains and adjoining areas).

and others, l979; Steven, Cunningham, and Anderson, l984; Steven, Rowley, and Cunningham, 1984), various geophysical studies (Campbell and Flanigan, l982; Earth Sciences Laboratory, l978; Flanigan and Campbell, l98l; Ross and others, l982), radiometric maps (Schutter and others, 1989), geochemical investigations (Miller and others, l984a,b,c), studies of ore deposits (Beaty and others, l986; Cunningham, Rye, and others, l984; Cunningham and Steven, l979b,c,d; Steven, l984; Steven and others, 1981; Steven, Cunningham, and Anderson, 1984), and a mineral resource appraisal (Steven and Morris, l986). More recent work bearing on the study area includes additional geologic mapping (Rowley and others, 1987; Anderson and others, 1990a,b), ore deposit and geochemical studies (Cunningham and others, 1994, 1997; Cunningham, Rassmussen, and others, 1998; Cunningham, Unruh, and others, 1998), and tectonic summaries (Anderson and Barnhard, 1992; Rowley and others, 1998; Rowley, 1998).

This report presents a color aeromagnetic map at scale 1:100,000 of the Tushar Mountains and surrounding areas (hereafter called the study area; map *A*, map sheet). Map *A* shows much more detail than the earlier aeromagnetic map of the study area (Campbell and others, 1984), which was flown with wider line spacing. This report also presents a 1:100,000 scale color map of complete Bouguer gravity anomalies in the study area (map *B*, map sheet). A colored geologic map of the study area at this same scale has been compiled by Rowley and others (in press); that geologic map (I-2645-A) is a companion map to this report (I-2645-B), and should be used together with it. This report also describes the gravity and aeromagnetic signatures of particular geologic features in the study area and presents density, magnetic susceptibility, and natural remanent magnetization (NRM) measurements made on 88 samples of igneous rocks. Small-scale versions of regional aeromagnetic (figs. 2 and 3, map sheet), topographic (fig. 4, map sheet), and geologic maps showing structures and alteration patterns (figs. 5 and 6) of the study area are included. Detailed versions of these maps have been published at l:50,000 scale (geology: Cunningham and others, l983; altered rocks: Cunningham, Steven, Rowley, and others, l984; gravity: Cook and others, l984; aeromagnetic data from an earlier survey: Campbell and others, l984), and these maps can be used for details.

REGIONAL GEOLOGIC SETTING

PIOCHE-MARYSVALE IGNEOUS BELT

The Pioche-Marysvale igneous belt (fig. 1) comprises an east-northeast-trending series of Oligocene, Miocene, and post-Miocene volcanic rocks and intrusions in southeastern Nevada and southwestern to south-central Utah. These igneous features include the Indian Peaks caldera complex (IPCC, figs. 2 and 3; Best and Grant, 1987; Rowley and others, in press) northeast of the town of Pioche, Nev., and the Marysvale volcanic field, which surrounds the town of Marysvale, Utah, as well as many igneous centers in between. Definitive boundaries of the Pioche-Marysvale belt are, to an extent, uncertain; by common agreement, it should include areas of observed volcanic and plutonic units that crop out at the surface, as well as intrusions that may be present at depth but can only be inferred. In their study of the Richfield, Utah, quadrangle, Steven and Morris (1986) drew boundary lines around areas with igneous outcrops of different ages; one of these boundaries (RBIC, surrounding Oligocene and lowermost Miocene calc-alkalic igneous centers) is reproduced on figures 2 and 3.

Because most large igneous deposits in the Western United States give rise to aeromagnetic anomalies, it is reasonable to ask whether the Pioche-Marysvale belt can be defined by aeromagnetic criteria. Figure 2 is a regional aeromagnetic map, on which a series of regional magnetic highs is apparent along the Pioche-Marysvale belt. On this map a parallel belt of magnetic lows occurs just north of the highs; these could be polarity lows, an expected part of the magnetic signature of bodies having induced magnetism. The phenomenon of polarity lows keeps magnetic highs from falling directly over their source bodies. In order to disperse the polarity lows, the observed fields are analytically reduced-to-pole (RTP), as in figure 3. An RTP magnetic map is one step removed from the observed data and can lead one astray when interpreting bodies that have strong magnetic remanence. Used with caution, however, and subject to field checking, RTP maps can be useful for making generalized interpretations. As mentioned above, the magnetic highs on RTP maps fall over their source bodies, so that by tracing a contour one can draw an outline parallel to the (depth- and susceptibility-weighted) edge of a source body. Such outlines will usually locate either plutons or sequences of normal-magnetic-polarity volcanic rocks. For a general discussion of the RTP process,

see Blakely (1994).

The RTP process has shrunk the continuous band of polarity lows north of the Pioche-Marysvale belt to a smaller low just north of the RBIC boundary in the present study area (fig. 3). Other RTP lows are also seen to the south of the Pioche-marysvale belt. Such lows commonly reflect basalts or other mafic volcanic rocks that have reversed magnetic polarity. As discussed below, we think basalts and tuffs having strong reversed magnetic polarity may be present in both the northern and southern parts of the study area. Such rocks may not be so prevalent along parts of the Pioche-marysvale belt where RTP processing has dispersed the aeromagnetic lows.

MARYSVALE VOLCANIC FIELD

The Marysvale volcanic field has a geologic history similar to that of many other volcanic fields in the Western United States. It contains early-erupted, voluminous, intermediate-composition, calc-alkaline volcanic rocks of middle Oligocene to earliest Miocene age that were followed by a bimodal assemblage of alkali rhyolite tuff and lava flows and local basalt flows, mostly of Miocene age. Throughout its igneous history, sporadic ash-flow eruptions resulted in the formation of calderas (fig. 5).

The intermediate-composition volcanic rocks were erupted from just before 30 Ma to about 22 Ma from scattered to clustered volcanoes. In the Tushar Mountains most of these rocks are hornblende-biotite-bearing calc-alkalic rocks of the Bullion Canyon Volcanics. Eruption of the Three Creeks Tuff Member of the Bullion Canyon Volcanics at 27 Ma resulted in the Three Creeks caldera (Steven, l98l) in the southern Pavant Range. Near the end of intermediate-composition volcanism, the eruption of the Delano Peak Tuff Member of the Bullion Canyon Volcanics led to the Big John caldera (Steven, Cunningham, and Anderson, l984), and the eruption of the Osiris Tuff, also near 23 Ma (Rowley and others, l988a,b), led to the Monroe Peak caldera.

The most voluminous rocks in the bimodal suite are the crystal-poor alkali-rhyolite ash-flow tuff units and lava flows of the Mount Belknap Volcanics (Cunningham and Steven, l979a; Budding and others, l987). The widespread Joe Lott Tuff Member is a variably welded ash-flow tuff unit whose eruption resulted in the Mount Belknap caldera. The eruption of the Red Hills Tuff Member of the Mount Belknap Volcanics resulted in the small Red Hills caldera. The mafic end member of the bimodal suite is represented by many lava flows derived from scattered sources. The earliest mafic flows to be erupted, at about 22 Ma, are potassium-rich (shoshonites), whereas later mafic flows are more normal basalts or basaltic andesites (Best and others, l980).

Altered rocks belonging to both the older and younger rock assemblages are widespread in the volcanic field and are commonly associated with known ore deposits or with potentially mineralized areas (Steven and Morris, 1986; Cunningham and others, 1994). Many of the intermediate-composition rocks in the central part of the study area (discussed below) have been pervasively propylitically altered. Argillic and advanced argillic alteration that resulted in replacement alunite deposits north and northeast of Marysvale took place at 23-22 Ma (Cunningham, Rye, and others, l984; Beaty and others, l986). Most of the alteration in the vicinity of Alunite Ridge, including vein alunite, is genetically associated with an unexposed stock (Cunningham, Rye, and others, 1984; Cunningham and others, 1997; Beaty and others, 1986), and took place at 14 Ma.

The Tushar Mountains and adjoining areas are in the High Plateaus subprovince, which forms the transition between the Colorado Plateau and the Basin and Range provinces. Most of the northerly striking major faults in the area (fig. 6) are basin-and-range structures. Most of the present topography reflects basin-range block faulting that was developed at 8-5 Ma (Steven and others, l979; Rowley and others, l98l). East-striking structural elements have been noted in the study area as well as in other parts of the High Plateaus and Great Basin. These elements include easterly striking faults and folds as well as easterly alignments of intrusions, volcanic centers, mineral deposits, hydrothermally altered areas, geophysical anomalies, and springs. These observations lead to the definition of "transverse zones," some of them hundreds of kilometers long, that formed generally parallel to the extension direction synchronously with Cenozoic (of basin-and-range and older episodes) normal faults that are oriented generally perpendicular to the extension direction (Rowley and others, 1998; Rowley, 1998). Two such zones, the Cove Fort transverse zone and the Blue Ribbon transverse zone, bound the central domain (fig. 5) of the Marysvale volcanic field and extend well to the west (figs. 2 and 3).

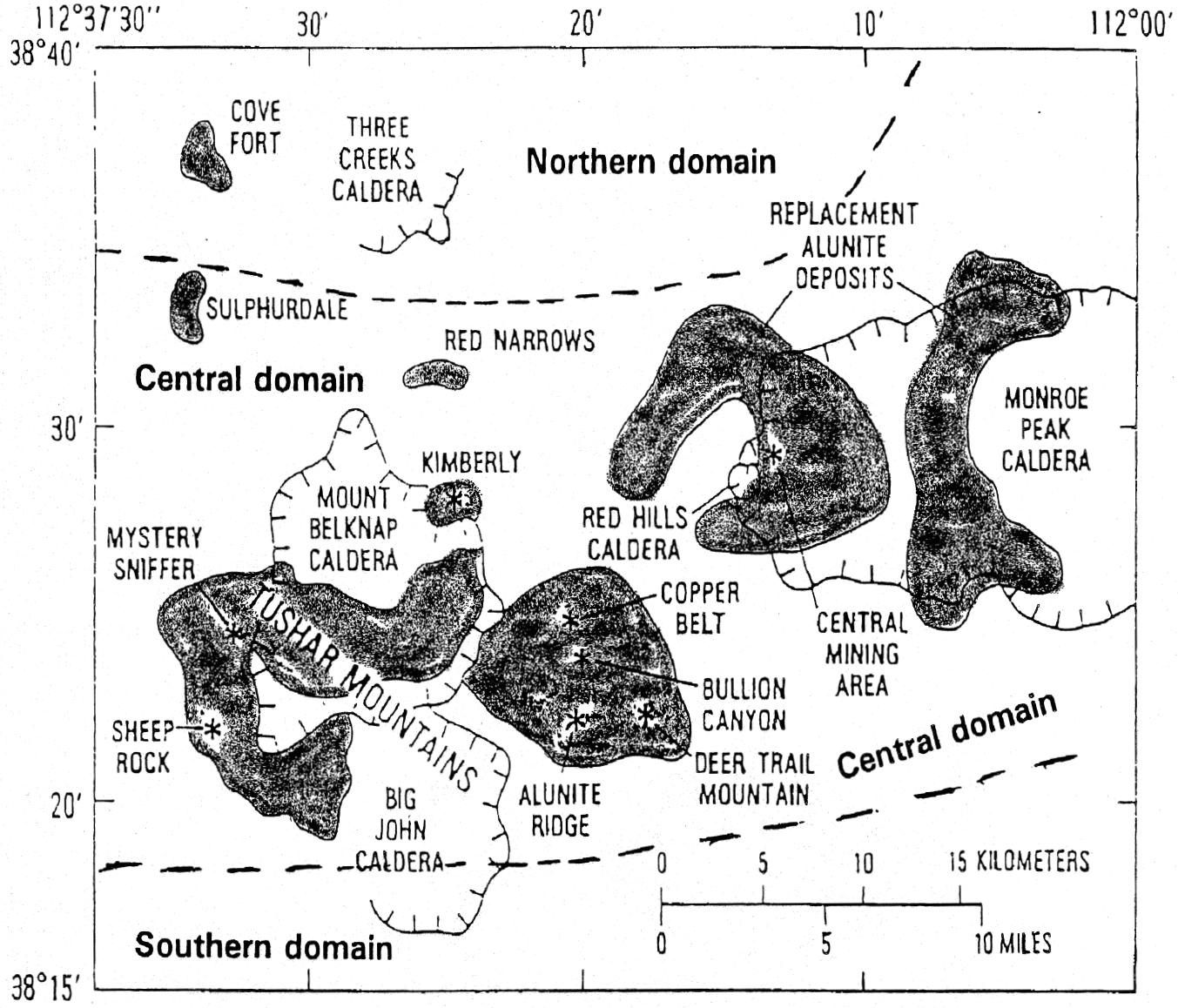

Figure 5. Schematic geologic map of the central Marysvale volcanic field, Utah, showing general locations of caldera walls (hachures on inside), altered areas (shaded areas), and selected mines and mining areas (asterisks).

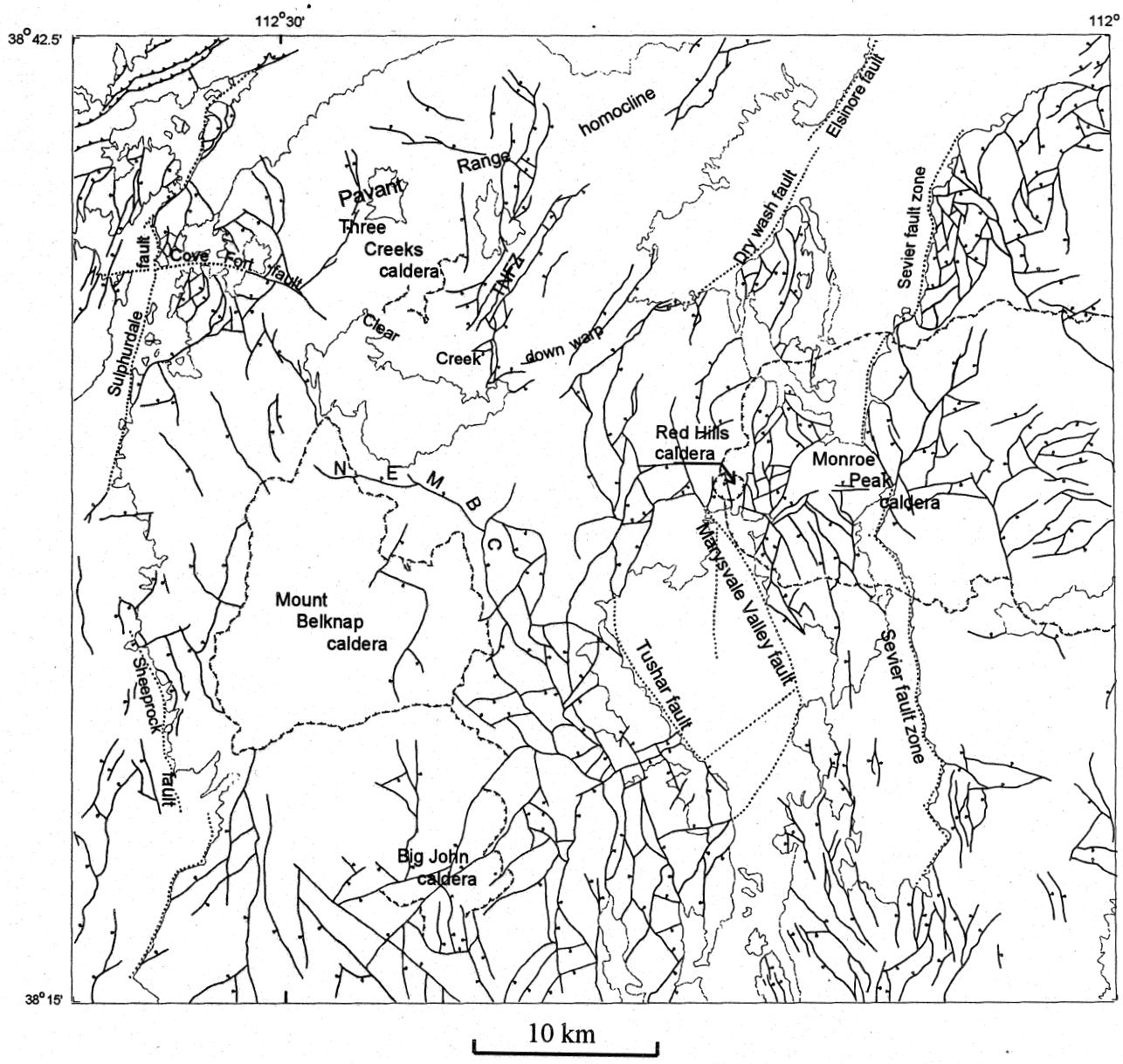

Figure 6. Geologic map overlay for the central Marysvale volcanic field, Utah, showing selected mapped faults (heavy lines, bar and ball on downthrown side of normal faults) and inferred faults (dotted lines), borders of Quaternary deposits (lighter lines), and boundaries of major calderas (hachured lines). TNFZ, The Narrows Fault Zone; NEMBC, arcuate faults northeast of Mount Belknap caldera. This map, minus place names, is the overlay for figures 10 and 11, and maps *A* and *B*.

DENSITY AND MAGNETIC PROPERTIES

DATA ACQUISITION

Dry bulk density, magnetic susceptibility, and natural remanent magnetization (NRM) were measured on samples of 88 igneous rocks representing the time-space-composition variations in igneous rocks of the Marysvale volcanic field (table 1). Preliminary data were reported in Mackie and Cunningham (1982), but magnetic properties were re-measured for this report. The measurements and sample localities are listed in table l, and lithologic descriptions of the rock units cited there are given in table 2. The results are graphically portrayed in figures 7-9, with statistics given in table 5.

Dry bulk density of fist-sized samples was measured by the buoyancy method (Johnson, l979). Samples were weighed dry (dry weight=W_d), then saturated with water in a vacuum chamber for 48 hours, and then weighed while submerged in water of density ρ_w (submerged weight=W_w). The bulk volume (V_b) was determined by $V_b=W_w/\rho_w$, and the dry bulk density (ρ_b) was determined by $\rho_b=W_d/V_b$.

Magnetic susceptibilities and NRM values were measured on dry chips of each sample, about 1 cm^3 in size, in the USGS Paleomagnetic Laboratory, Denver, Colo. The chips were spalled off the larger samples as gently as possible to avoid changing NRM by mechanical shock, and it is thought that errors from this possible cause are small. Susceptibilities were measured at a frequency of 600 Hz in a small calibrated coil having an induction field of 0.1 millitesla. NRM values were measured at 90 Hz with a spinner magnetometer having a sensitivity < 1.0×10^{-5} amperes/ meter. The Koenigsberger Q, the dimensionless ratio of NRM (permanent) to induced magnetization, was calculated for each sample by dividing measured NRM (in emu/cm^3) by an induced magnetization value found by multiplying the measured susceptibility (cgs system) by 0.54 oersted, a value that represents the general magnitude of the Earth's magnetic field in the study area.

Susceptibility and NRM for 5 of the 88 samples were measured twice, using different chips from the same original sample. Table 4 gives the results for these duplicate samples. All the repeated susceptibilities were within a few percent of each other. The NRM values, however, were not. The two NRM values for samples M859, M930D, and 79-1518 differed by 6-9 percent, while those for sample 79-1517 differed by 35 percent and those for sample M798 were different by a factor of almost 2. Differences in Q were similar, reflecting the NRM variations that went into the Q calculation. We think that most of these differences represent genuine variations in magnetic properties from place to place within the rock sample itself. In turn, this means that all NRM and Q values cited below should be regarded as samples from a distribution of values in the parent rocks that may vary by as much as, perhaps, a factor of 2. Note, though, that this likely variability is diminished by using logarithms of the measured values, which we do below. For cases of duplicate samples, values given in table 1 and in figures 7-9 were those for the chip having the **larger** NRM.

DISCUSSION OF DENSITY AND MAGNETIC PROPERTIES

Because this set of sample measurements is quite extensive, we used it to look for systematic differences between rock types and for correlations between the different physical properties that were measured. The samples were divided by rock type into classes (table 3). One division was between extrusive rocks (denoted X or OX) and intrusive rocks from the study area (I). X and OX rocks were subdivided into extrusive rhyolites (-R), dacites and other intermediate composition rocks (-D), basalts and other mafic composition rocks (-B), and tuffs. The tuffs were further divided according to their degree of welding: poorly welded (-TP), moderately welded (-TM), and densely welded (-TD). I rocks were subdivided into intrusive rhyolites (-R), granitic rocks (-G), and monzonites (-M).

Rocks in many parts of the study area have been pervasively propylitically or argillically altered. Therefore, another division of samples was made to indicate degree of alteration. Unaltered or fresh samples were denoted U. Samples of rocks that are propylitically altered were denoted as "slightly altered" (S). Samples that are at least partly argillically altered were termed "moderately altered" (M), and rocks that have been subjected to advanced argillic alteration, especially where alunite has been formed, were termed "highly altered" (H). The rocks were subdivided into those of the Bullion Canyon Volcanics (denoted -BC) and Mount Belknap Volcanics (-MB). The X class mentioned above denotes extrusive rocks of the -BC and -MB suites, and OX denotes extrusive rocks that are neither -MB nor -BC. Class -BC includes seven samples that are, in fact, from units of the Monroe Peak caldera (Rowley and others, in press); these have been

included with true Bullion Canyon Volcanic rocks because of their petrological affinities and similar ages. Note that class I includes eight samples of Bullion Canyon Volcanic rocks that are **intrusive** in nature.

The measured susceptibilities of five of the highly altered samples turned out to be small but **negative**. These five samples were not used in making the graphs that show susceptibility and Koenigsberger Q, or in the statistical analyses (below) of susceptibility and Q. Negative susceptibility values suggest that all induced magnetic domains have disappeared in those samples — essentially, their crystal structure has been so disrupted that it does not support a bulk induced magnetization, and the remaining measured value comes from the molecular/atomic level. This negative, or diamagnetic, susceptibility is present in all matter, but is usually masked by the stronger effects of crystalline structure.

Figure 7 shows histograms for the resulting measurements. Shading patterns of the histogram boxes indicate degree of alteration (H, M, S, and U) for extrusive rocks of the Bullion Canyon Volcanics and Mount Belknap Volcanics, with the remaining samples aggregated together as either other (non -BC or -MB) extrusive rocks or intrusive rocks. Histogram intervals are linear for the density graph, but logarithmic for the susceptibility, NRM, and Koenigsberger Q graphs. The logarithmic intervals reflect the fact that the magnetic property values spread over many orders of magnitude, and they suggest that these three physical properties may be distributed log-normally.

The density histogram (upper left panel, fig. 7) shows that most of the low-density samples are altered Bullion Canyon or Mount Belknap Volcanics. All the other samples in the low-density group (< 2.26 g/cm^3) are ash-flow tuffs. High density samples (> 2.6 g/cm^3) are generally intermediate- and mafic-composition extrusive rocks and intrusive rocks, all but one of them (M330) monzonites. The one highly altered sample in the high-density group is M53, which consists of a tightly meshed intergrowth of alunite (density about 2.7 g/cm^3) and quartz.

The susceptibility and NRM histograms (upper right and lower left panels, respectively, fig. 7) show similar trends. As with density, altered samples of Bullion Canyon and Mount Belknap Volcanics generally fall in the lower ranges of both histograms (< 1.0E-05 cgs for susceptibility, and < 2.5E-05 emu/cm^3 for NRM). One unaltered sample, M583, a rhyolite of the Mount Belknap Volcanics, falls in the low range for both susceptibility and NRM. Sample M91, a moderately welded tuff of the Mount Belknap Volcanics, also falls in the low range of susceptibility. Most tuffs, though, have medium susceptibility and quite high NRM. As with density, samples of intermediate- and mafic-composition extrusive rocks and intrusive rocks, especially monzonites, tend to fall in the high ranges of the susceptibility and NRM histograms (> 1.4E-03 cgs for susceptibility and > 1.0E-03 emu/cm^3 for NRM). Sample M739, a densely welded mafic tuff of Albinus Canyon, also falls in the high-susceptibility range. Besides the intermediate- and mafic-composition extrusive and intrusive rocks cited above, the high range of the NRM histogram contains many samples of moderately and densely welded tuffs (M928, M908, M520, M75, M472, M859, and M145B, listed in order of increasing NRM) and two other samples, M581 and M263. M581 and M263 were collected near the summits of Mount Baldy and Delano Peak, respectively, so that their high NRM values may have resulted from lightning strikes on those peaks sometime in the past. Other samples collected from high elevations, so that they could also have been struck by lightning, include M145B, M859, and M903. Lightning strikes typically raise NRM values, sometimes by as much as 2 orders of magnitude, but seldom or never **decrease** them (J. Rosenbaum, U.S. Geological Survey, oral commun., 1998). Therefore, possible lightning strikes could have biased the histograms for NRM, and consequently for Q, **upward**.

Except for the comments about lightning strikes, the above generalizations do not seem to hold for the Koenigsberger Q values (lower right panel, fig. 7).

Figure 8 shows how well physical properties correlate with each other. Correlation coefficients r were calculated for all pairs of physical properties; r equals 1.00 if the variables are perfectly correlated, -1.00 if they are perfectly anti-correlated, and 0.00 if they are uncorrelated. There is a fair correlation (r=0.58) between density and the logarithm of susceptibility (fig. 8, upper left panel), which improves only slightly (r=0.60) if the altered samples are not used. There is good correlation between log NRM and log susceptibility (fig. 8, upper right panel; r=0.81 for all samples, but r=0.56 for fresh samples only), and a poor correlation between log NRM and density (fig. 8, lower left panel; r=0.49 for all samples, r=0.32 for fresh samples only). There is no correlation between Q and density (fig. 8, lower right panel; r=0.03 and -0.01). As would be expected because Q is calculated from both NRM and

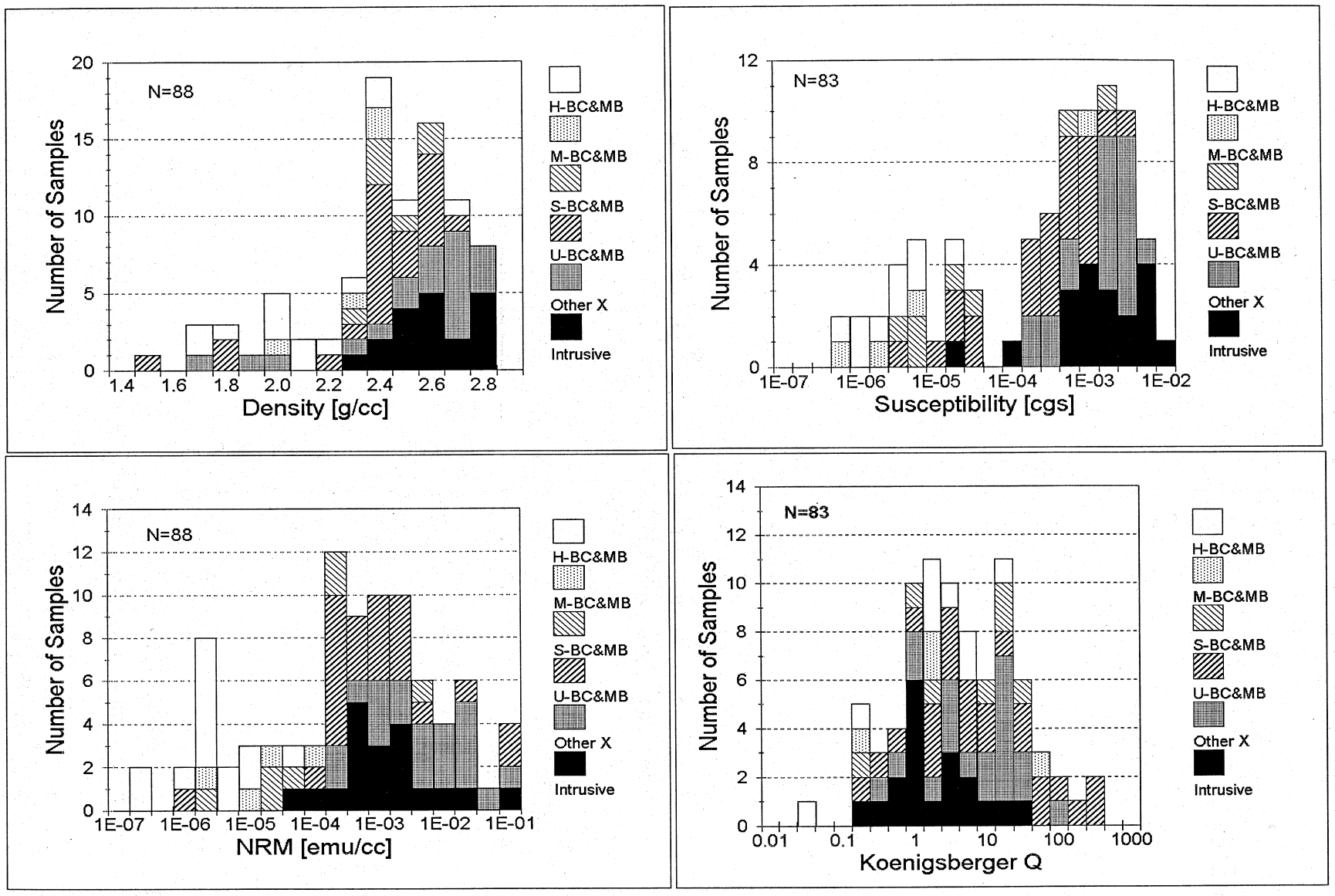

Figure 7. Histograms of physical properties measured on rock samples from the Marysvale volcanic field, Utah. Abbreviations are explained in table 3. 1 cc = 1 cm^3. E denotes exponential; that is, 1E-04 = 1.0×10^{-4}.

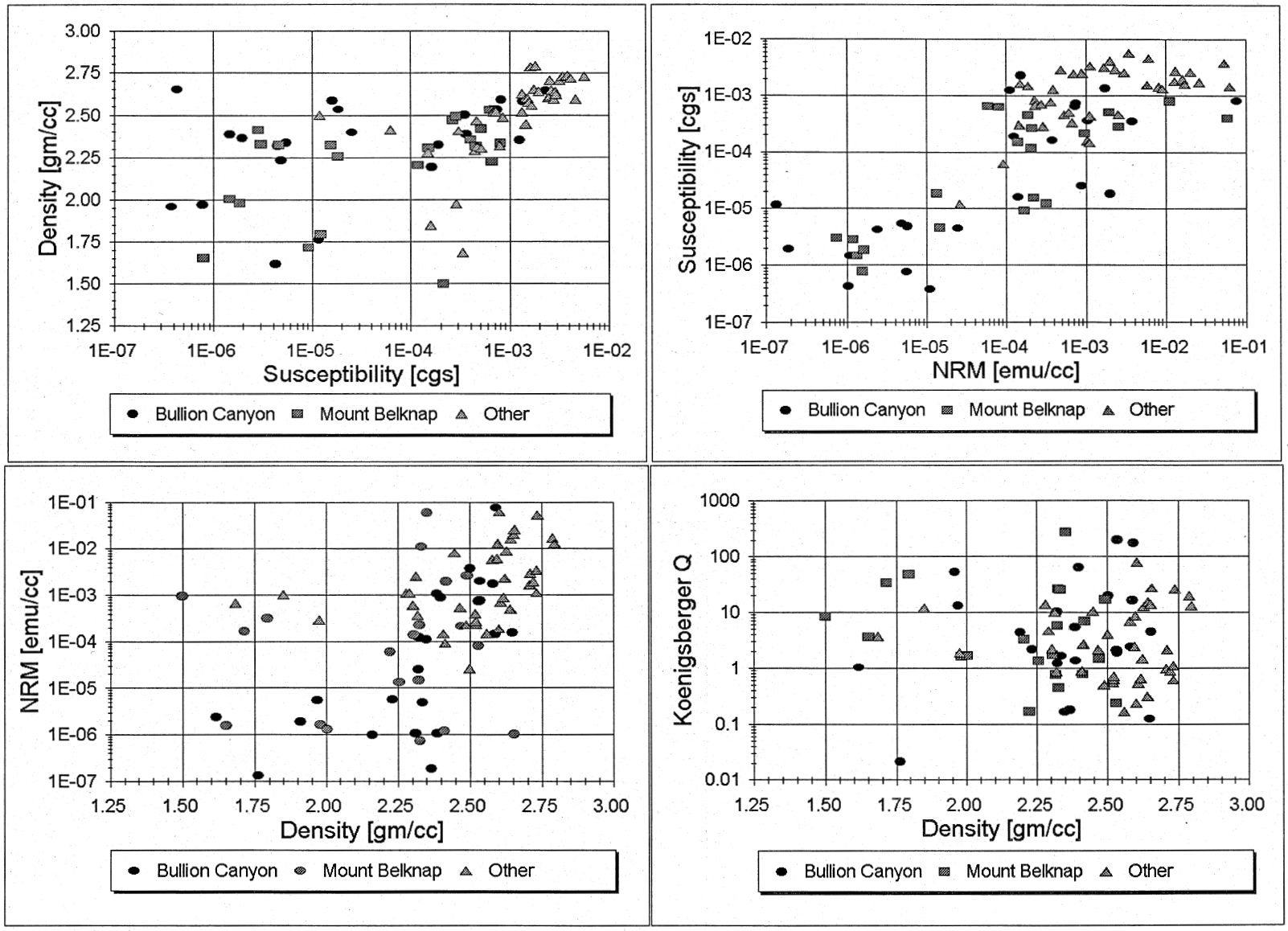

Figure 8. Graphs of correlations between different pairs of physical properties measured on rock samples from Marysvale volcanic field, Utah. 1 cc = 1 cm^3. E denotes exponential; that is, 1E-04 = 1.0×10^{-4}.

susceptibility, log Q correlates to some extent with both (r=0.51 and 0.62 for log NRM and r=-0.09 and -0.31 for log susceptibility; not shown on fig. 8).

Simple statistical analysis was done on physical properties of extrusive rocks of the Mount Belknap and Bullion Canyon Volcanics with various degrees of alteration (H, M, S, and U). To investigate variables such as degree of welding of tuffs and composition of the extrusive rocks, however, it was appropriate to combine unaltered -MB and -BC samples with the samples designated OX. All 30 of the U-MB and U-BC samples, therefore, were reclassified as an appropriate X-type sample and used in making statistical calculations for the X- sample populations. Sample M91, for example, consisted of fresh, moderately welded tuff of the Mount Belknap Volcanics, and so it was used in analysis of both classes U-MB and X-TM.

Table 5 gives statistics for each sample class. The columns labeled "Min" and "Max" give the smallest and largest, respectively, of the measured values in the class. The column labeled "N" gives the number of samples in the class. To get statistics that will reliably estimate true means and standard deviations for the underlying distributions, standard textbooks (for example, Spiegel, 1961, p. 188) recommend that N should be greater than 30. All our classes have far fewer samples than that; three, in fact, only have a single sample. Note, therefore, that the means, m (listed in table 5), and standard deviations, SD (not listed as such, but used in making table 5), are means and standard deviations **of the sample**, and may represent quite poor estimates of the means and standard deviations **of the population**. The lightly shaded column contains sample means, m. Because samples are so few, we need some way to tell how well this sample mean may estimate the "true" mean of the underlying distribution. This is done using standard error of the mean, SE: the true mean is likely, at some appropriate confidence level depending on N, to fall within one SE of the sample mean. The resulting values in table 5 are arranged in what ought to be ascending order from observed minimum to maximum values, with the sample mean and the predicted range delimiters for the true mean (m-SE and m+SE) in the middle. In some cases, however, the ascending order fails, and SD's fall outside the range of actually measured values. In constructing table 5 we assumed that the **logarithms** of susceptibility, NRM, and Q (rather than the values themselves) are normally distributed; the statistics were accordingly calculated using the logarithms of the measured values, and the values labeled m, $m \pm SE$, and $m \pm SD$ in table 5 represent appropriate antilogs.

Figure 9 presents bar-and-box charts to show how the four physical properties we measured change with alteration state and lithology. In these charts, the vertical bars show the total range of measured values for that sample class, and the boxes show the standard error of the mean. Each "true" mean, in other words, ought to fall somewhere inside its box. If more samples were used in a class, our estimate of its true mean would probably improve, and its box on these charts would shrink. Note that figure 9 does not show SD values (table 5), which estimate the underlying distributions. Ideally, the sizes and positions of boxes representing standard deviations, if they were shown, would not change very much as more samples were measured and used.

GENERALIZATIONS ABOUT DENSITY AND MAGNETIC PROPERTIES

Degree of alteration of rocks of the Bullion Canyon and Mount Belknap Volcanics

Densities of rocks of the Bullion Canyon and Mount Belknap Volcanics decrease with degree of alteration: the more altered, the less dense. As alteration progresses from fresh through propylitic, argillic, to advanced argillic, mineralogic changes reflect both gain and loss of chemical components. The bulk density of a rock typically decreases as the degree of hydrothermal alteration increases, mostly because there is a concurrent net loss of chemical components and an increase in pore space. As mentioned above, though, some of our samples do not fit this systematic trend; these include fresh poorly to moderately welded ash-flow tuffs containing visible pumice fragments (such as M91 and M94), or highly altered rock samples containing large amounts of alunite (M53).

Although the sample ranges overlap substantially, **on average** rocks of the Mount Belknap Volcanics are less dense than those of the Bullion Canyon Volcanics with corresponding degrees of alteration. They also have lower susceptibilities, on average, and (at least for fresh rocks) lower NRM. These differences are attributed to the facts that the Bullion Canyon assemblage of rocks is more mafic and the Mount Belknap assemblage of rocks is more silicic.

Unlike density, which increases as alteration decreases, both susceptibility and NRM for almost all degrees of altered rocks are lower than those of fresh

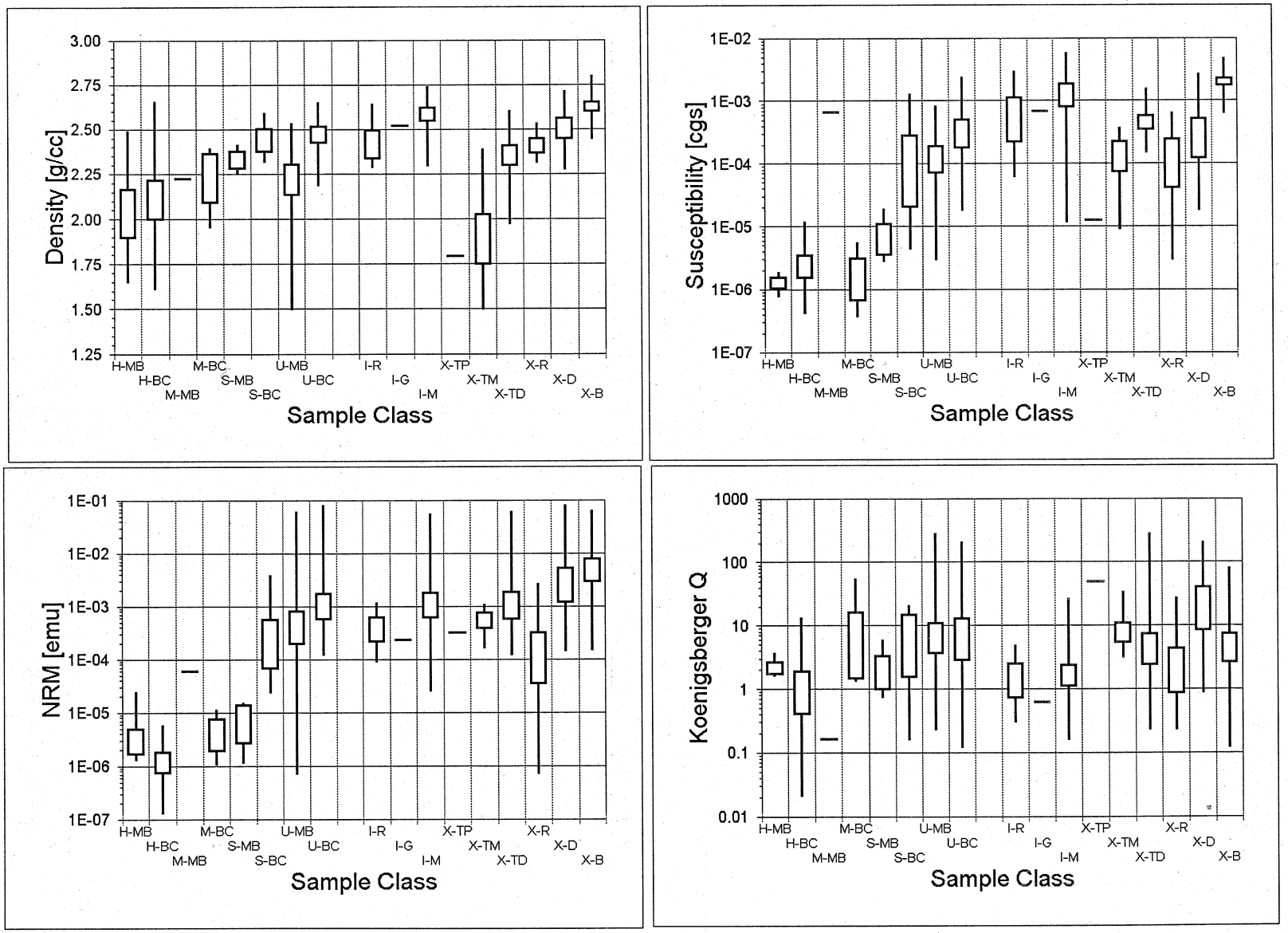

Figure 9. Graphs of statistical means (boxes) and extremes (bars) for physical properties measured on rock samples from Marysvale volcanic field, Utah. Single line denotes only one sample in the class. Abbreviations are explained in table 3. 1 cc = 1 cm^3. E denotes exponential; that is, 1E-04 = 1.0 ×1 0^{-4}.

rocks by at least a factor of 10. Bullion Canyon Volcanic rocks that are only slightly altered, however, must be exempted from this statement: they have susceptibility and NRM values that are comparable to those of fresh Mount Belknap Volcanic rocks. As with density, these differences may reflect general differences in composition between the two rock assemblages. For most rocks in this suite, mafic index will correlate with magnetite content, which, in turn, will account for most of the magnetic properties. As the degree of alteration increases, magnetite becomes oxidized to hematite or hydrated to limonite. This magnetite conversion presumably is complete in all moderately and highly altered samples but may only be incipient in many of the slightly altered Bullion Canyon Volcanic rock samples. We see that, except for slightly altered Bullion Canyon Volcanics, all altered volcanic rocks in the study area have relatively low magnetizations compared with fresh volcanic rocks. Therefore, we expect areas containing large amounts of altered rocks to show lower anomalies on an aeromagnetic map than will areas of fresh volcanic rocks.

There is only one sample (M223) in class M-MB, and both its susceptibility and NRM are very high compared to those of other altered samples. The M223 chip resembles an altered rhyolite, for it is bleached a uniform white. Examination of the sample with a hand lens, however, shows that it contains many tiny fragments of a black mineral. We infer from the high values of susceptibility and NRM for sample M223 that this mineral is finely disseminated magnetite.

Koenigsberger ratios, Q, do not vary in any clear way with degree of alteration. This does not change our conclusion that altered rocks have negligible magnetizations, however: if both NRM and susceptibility are negligibly small (as in most altered units), then the rock is effectively nonmagnetic and its Q is irrelevant.

In interpreting gravity and magnetic maps it can be useful to have a framework of "typical" values of physical properties to refer to, however imprecise. Such typical values for rocks in the study area are listed in table 6. Table 6 must be used cautiously, in conjunction with the fuller set of values in table 5, and with the clear realization that the underlying suites of rocks vary continuously with respect to degree of alteration and composition. Our classifications have broken these underlying continuums into useful subgroups, but they are arbitrary.

Composition of intrusive rocks

Although their ranges overlap, on average, density, susceptibility, and NRM all increase slightly as one proceeds from intrusive rhyolites, through granite, to monzonites (table 6). This is as expected from increasing mafic indices and the higher iron and magnesium contents of monzonites.

Intrusive rocks have generally higher susceptibility and lower Q (especially granite) than most extrusive ones. Their lower Q probably reflects their slower cooling; hence, larger crystals and inter-crystal magnetic domains. Big magnetic domains that are not pinned by crystal boundaries are more susceptible to growth by magnetic induction.

Degree of welding of tuffs

On average, both density and susceptibility of tuffs increase markedly with their degree of welding, and NRM probably increases somewhat (table 6). Tuffs, like other rapidly cooled volcanic rocks from the Marysvale volcanic field, have generally high Q.

Composition of extrusive rocks

On moving from extrusive rhyolites, through intermediate-composition extrusive rocks, to mafic-composition extrusive rocks, susceptibility and NRM substantially increase, and density moderately increases (table 6). Again, this is in line with increasing mafic index and likely corresponding increase in magnetite content. The mafic extrusive rocks (class X-B) have, on average, the highest density, susceptibility and NRM of all the rock classes analyzed.

Koenigsberger ratios

Most of the above generalizations agree with what we expect from general principles, and so are reassuring but not surprising. Probably the most important lesson from figure 8 is that, **on average**, all volcanic rocks from the Marysvale volcanic field have high Q, generally in the range from 2 to 10. Their remanent (paleomagnetic) magnetizations, in other words, will be 2-10 times stronger than those arising through induction by the present-day Earth's field. Hence, the magnetization directions that were frozen into the rocks when they cooled may still be prevalent today, overpowering the induced magnetizations that align with the direction of the present Earth's field. We were not able to measure

these directions, for our samples were not oriented. In principle, the vector sum of the two magnetizations in high-Q rocks could point in any direction. In practice, however, Tertiary volcanic rocks in the Western United States tend to have net magnetization directions that are roughly aligned either **with** the present Earth's field direction (normal magnetization direction) or **against** it (reversed magnetization direction; see, for example, Bath, 1968). During Oligocene through Holocene time, the Earth's field has been reversed about half of the time (Geological Society of America, 1984), so that reversed magnetizations should be common. This means that extreme lows on the aeromagnetic map, particularly if they fall over thick flow sequences, likely reflect reversed magnetizations in those flows.

SOURCES OF GEOPHYSICAL DATA

AEROMAGNETIC DATA SOURCE

The aeromagnetic data shown on map *A* (map sheet; U.S. Department of Energy, 1982) were collected by Geodata International, Inc., under contract with the U.S. Department of Energy (DOE) as part of the National Uranium Resource Evaluation (NURE) program. Nominal survey altitude was 122 m above ground level. The flight lines were oriented east-west at a nominal line spacing of 400 m; three north-south tie lines were spaced 12-20 km apart. The main purpose of the survey was to collect detailed spectrometric radiometric data over the Marysvale volcanic field, an area of many uranium prospects. As for most NURE studies, aeromagnetic data were collected incidentally to the radiometric data. The radiometric data have been reprocessed and presented at 1:100,000 scale by Schutter and others (1989). This NURE survey area is almost, but not quite, the same as the area of the companion geologic map by Rowley and others (in press); so as to facilitate comparison with that geologic map, the area of map *A* was made coincident with it. The colored part of the map shows the NURE survey area.

The aeromagnetic data on map *A* are those supplied to DOE by the contractor. The close line-spacing of the original survey, the sensitivity of the magnetometer used to collect the data (thought to be 1-2 nanotesla, nT), and the wide range of observed magnetic fields in the study area make for a good level of detail on this data set. In order to preserve such detail insofar as possible, we felt it best to show contractor-supplied survey data on map *A*, and not attempt to correct possible blemishes by further processing.

Figure 10 (map sheet) is a key to map *A*, showing the aeromagnetic data in color-shaded relief form. In this presentation, the aeromagnetic map is treated as a topographic surface, and is illuminated by a computer-driven "sun" that casts shadows. The sun in figure 10 is at an elevation of 60° and azimuth of 180°. The scene is illuminated from due south, in other words, perpendicular to the flight lines, an orientation that highlights certain blemishes in the data set. In particular, this orientation will show up problems in "leveling" the flight lines. If the survey aircraft flies too high, the aeromagnetic fields it measures will be somewhat weaker than if it were at correct altitude; if too low, they will be somewhat stronger. To correct for this, data from each flight line are shifted down or up (leveled) so that the final composited survey will show fields that vary smoothly from one flight line to the next. Imperfect leveling will show up as shadows along flight lines on a color-shaded-relief map.

Figure 10 shows some flight-line shadowing; this alerts us to be wary of apparent east-west-aligned features on map *A*, which may be caused all or in part by flight-line-related artifacts. In particular, there are two places on the map (**strip A** and **strip B** on fig. 10) where apparent leveling problems persist. Both involve two or more adjacent flight lines that appear to be properly leveled with respect to each other, but that seem to have field values that are too low (**strip A**) or high (**strip B**) with respect to nearby flight lines.

Strip A (fig. 10) extends from the southern part of the Mount Belknap caldera east to the south-central Marysvale Valley. This strip appears to have been misleveled such that fields along it came out some 25-50 nT (that is, 1-2 color contours on map *A*) low. In particular, one should mentally discount the obvious east-west-trending aeromagnetic gradients at about lat 38°23' N. connecting the low in the southern part of the Mount Belknap caldera with that in the Marysvale Valley. No such feature occurs on an earlier aeromagnetic map of the area (see below), so it is almost certainly a data-processing artifact.

Strip B (fig. 10) extends from the northernmost apex of the Mount Belknap caldera eastwards for about 15 km. Fields in this strip appear to be as much as 50-100 nT (that is, 2-4 color contours on map *A*) too high. The **east-trending** band of lows just south of **strip B** (labeled "**rn**"; discussed below) appears on an earlier aeromagnetic map that had north-south flight lines (Campbell and others, 1984), so we may

infer that it is **strip B** that is misleveled, rather than the **rn** low. High **Y** appears on both maps, so it is not clear whether the **strip B** mislevel extends that far to the east. This interpretation is complicated, however, because the older map does show a minor high elongated to the east in about the middle third of **strip B**, and a corresponding high is seen to extend above local magnetic background on map *A*. Thus not all of the **strip B** high can be attributed to data-processing artifacts. Nevertheless, one probably should disregard the sharp east-west-trending aeromagnetic gradients on map *A* that define the north and south edges of **strip B**.

GRAVITY DATA SOURCES

Map *B* (map sheet) is a complete Bouguer gravity anomaly map of the study area, and figure 11 (map sheet) is a key to features on map *B* that are discussed herein. Map *B* was made using more than 2,300 gravity stations from the U.S. Geological Survey gravity files. In making complete Bouguer gravity maps, one must correct for the gravitational attraction of rocks under and near each gravity station. Such corrections assume a constant density value for all rocks in the study area, ideally the density of the "average" rock there. For regional gravity maps, it is customary to use a reduction density of 2.67 g/cc— the density of average crustal rocks. That density, however, is too high for rocks of the Marysvale volcanic field (fig. 7). Instead, a reduction density of 2.40 g/cm^3 was used in making map *B*.

Map *B* may be compared with gravity maps of the Richfield sheet (Cook and others, 1981) and of the state of Utah (Cook and others, 1975, 1989). A major characteristic of such regional gravity maps is that they strongly reflect basins (as gravity lows) and ranges (gravity highs). By making appropriate assumptions (Jachens and Moring, 1990), other gravity maps may be derived in which this basin-and-range effect is much reduced. Such "basement gravity" maps let us see gravity features that may have been masked by basin-and-range signatures (see Saltus and Jachens, 1995).

Bouguer slab formula

In discussing certain gravity anomalies below, we will use the Bouguer slab formula to estimate basin thickness. The formula for the gravity effect Δg of a flat infinite slab of rock having thickness T and anomalous density $\Delta\rho$ is:

$$\Delta g\ [\text{mGal}] = 41.89\ \ T\ [\text{km}]\ \Delta\rho\ [\text{g/cm}^3].$$

For bodies of rock that are slablike but not infinite in extent the right-hand side of this equation has an additional factor that reflects the geometry of the body. At gravity stations located over the center of a large anomalous body, however, this geometrical factor nearly equals 1.00, so the formula can be used to estimate the body's thickness, T. The density difference, $\Delta\rho$, represents the density of the body minus the density of surrounding rocks. A graph of this relation is shown in figure 12. As an example, a basin containing 300 m of sediments of density 2.2 but surrounded by rocks of density 2.4 will have a relative gravity anomaly of about 41.89 × 0.3 km × -0.2 g/cm^3 = -2.5 mGal. The minus sign says that the anomaly is a relative low.

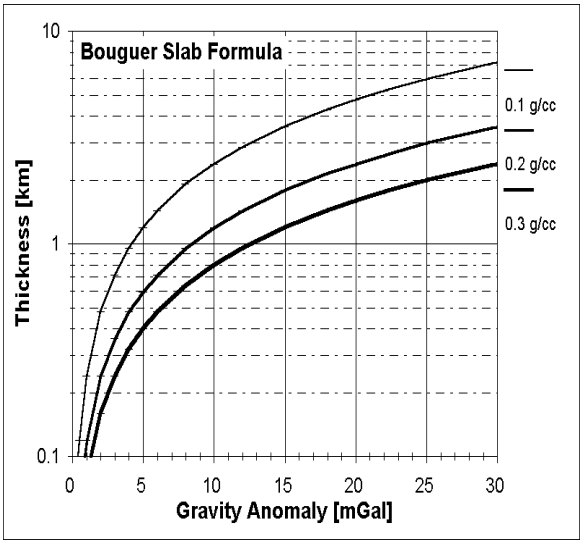

Figure 12. Bouguer slab formula graph, which can be used to estimate thickness of material, in km, needed to produce a given gravity anomaly. The different curves apply for density differences $\Delta\rho$ of 0.1, 0.2, and 0.3 g/cm^3, as labeled.

INTERPRETATION OF GEOPHYSICAL FEATURES

Gravity and magnetic expressions in themselves reflect only the intensities and spatial distributions of rock properties. By comparing them with geologic information, however, it is often possible to identify the source rocks by their anomalies and to make inferences about subsurface geology. In this

overview of the Tushar Mountains area, we focus on major features of the geologic (Rowley and others, in press; figs. 5 and 6), gravity (map *B*), and magnetic (map *A*) maps.

THREE GRAVITY AND MAGNETIC DOMAINS: A GENERALIZED DESCRIPTION

Broadly speaking, the study area can be divided on the basis of gravity and aeromagnetic maps into three east-northeast-trending geophysical domains (fig. 5). The southern domain includes about one-sixth of the study area and is an area of "birdseye" magnetics (closely interspersed highs and lows) and moderate gravity values. The central domain includes about half of the study area and is an area of generally high magnetic values and low gravity values. The northern domain includes the remaining one-third of the study area and is characterized generally by very low magnetic values and by gravity highs (more precisely, a southeasterly decreasing gravity gradient). These three domains generally reflect pre-basin-and-range tectonic and magmatic activity. Superposed on these domains are north- or north-northeast-trending features; on the gravity map these generally reflect basin-and-range tectonic events, but on the magnetic map they are largely due to boundaries of calderas that occupy the central domain.

The low gravity area of the central domain is part of a regional low that contains some of the lowest complete Bouguer gravity anomaly values in Utah (Cook and others, l975, l98l, 1989; Halliday and Cook, l980). This gravity low corresponds to the Marysvale volcanic field. Similar features in Colorado having corresponding outcrops of Tertiary extrusive and intrusive rocks have been interpreted to indicate the distribution of underlying batholiths (Plouff and Pakiser, l972; Tweto and Case, l972).

BASIN-AND-RANGE FEATURES

Several major basin-and-range fault zones in the study area are reflected on gravity and magnetic maps. These fault zones were especially active in latest Miocene time, 8-5 Ma (Rowley and others, l98l), when the present fault-block topography formed in this part of the High Plateaus. Extensional tectonism at this time formed a welter of faults throughout the study area (fig. 6); here we are concerned only with the major zones, those that bound major mountain masses or deeply subsided basins. Some of the major zones shown on figure 6 are observable as single fractures, but elsewhere they mark the approximate position of major displacement within a broader zone of distributed offsets. Other major zones are inferred from geophysical data rather than from surface geology. These are shown by lines of dots on the overlay map (fig. 6).

Pavant Range homocline

The Pavant Range, which occupies the north-central part of the map area north of the Clear Creek downwarp and west of the Elsinore and Dry Wash faults (figs. 4 and 6), consists of a south- to southeast-dipping homocline of volcanic rocks. Dips in the homocline vary from only a few degrees south in the vicinity of the Three Creeks caldera to as much as 15° southeast adjacent to the Elsinore fault. The homocline formed in latest Miocene time (7-5 Ma) during the main pulse of basin-and-range tectonism in this part of Utah (Rowley and others, l98l), when a dome some 80-l00 km across was pushed up. This dome, now collapsed, includes the Pavant Range and adjacent areas to the west and northwest (T.A. Steven and H.T. Morris, unpub. data, 1985); the Pavant range homocline represents its southern flank.

The Pavant Range homocline is reflected in the gravity data (map *B*) by a relatively smooth gravity gradient that decreases from about -l65 mGal near the northwest corner of the study area to about -200 mGal near the southeast margin of the homocline. Regionally, this gradient follows the southeast flank of the Pavant Range for a distance of at least 100 km, between the towns of Gunnison and Sulphurdale; it is relatively insensitive to topography, to the differences between volcanic and sedimentary bedrock, or to the presence or absence of significant alluvial fill. This regional-scale gravity gradient is thus presumed to reflect a major deep-seated source. In a review of regional geophysical parameters extending nearly across Utah, Thompson and Zoback (l979) interpreted this gradient to reflect the southeastern edge of an area in west-central Utah where crustal thinning has brought dense subcrustal rocks up to shallower levels. This interpretation accounts not only for the gravity gradient associated with the Pavant Range, but also for the doming and concurrent collapse of the distended near-surface rocks over a large area of regional gravity highs located to the northwest of the study area.

Clear Creek downwarp, Dry Wash and Cove Fort faults

The Clear Creek downwarp (fig. 6) is an east-trending, broad faulted syncline that extends between the Pavant Range and the Tushar Mountains. This feature had a long and complex history of development, extending from middle Oligocene at least to the end of the Miocene, so that it may predate development of the Pavant Range homocline, which now forms the northern limb of the syncline. The major Clear Creek downwarp displacement shown by surface geology took place during basin-and-range tectonism in latest Miocene time. Some of the gravity and magnetic trends within this downwarp do not have clearly recognized counterparts in the mapped geology, and they may reflect buried discontinuities related to the development of the downwarp.

The surface manifestations of the Clear Creek downwarp begin at its eastern end as a curving continuation of the Dry Wash fault. The Dry Wash fault bounds the southeastern margin of part of the Pavant Range homocline, and it is one of a series of northeast-striking, oblique slip (normal and left-lateral) faults (Anderson and Barnhard, 1992) along the west side of a deep fault trough between the upfaulted horst blocks of the northern Sevier Plateau and the Pavant Range (discussed in the next section of this report). The Dry Wash fault dips northwest and splits the fault trough into tilted blocks, whereas other faults farther north (for example, the Elsinore fault) dip east and define the west flank of a graben. The Dry Wash fault extends southwest from Clear Creek across the trend of the Clear Creek downwarp and dies out as shown on figure 6. (See discussion of Red Narrows area, below.)

At the east end of the Clear Creek downwarp, the major geologic displacement consists of an en echelon line of steep monoclines, down to the north. These monoclines end abruptly on the west approximately at The Narrows against a northeast-trending fault or fault zone (TNFZ on fig. 6); farther west the downwarp consists of a broad, open syncline that can be recognized to the crest of the mountains. From this point westward, the trend is marked by the Cove Fort fault, which formed before 23 Ma and thus was not part of the main late Miocene pulse of basin-and-range tectonism.

Gravity and magnetic trends along the Clear Creek downwarp reflect some of the geologic features described above. Deep gravity and magnetic lows just northwest of the northern part of Dry Wash fault (the Joseph Flats low, **jf** on figs. 10 and 11) reflects a tilted body of Miocene (l5-7 Ma) fluvial and lacustrine sediments of the Sevier River Formation (Rowley and others, 1994). While the **jf** gravity low probably reflects low-density Sevier River Formation sediments under Joseph Flats, the **jf** magnetic low may reflect more than merely nonmagnetic sediments. In particular, it is not erased by RTP processing (fig. 3), arguing that reversed-polarity volcanic flows (tuffs?) may floor the Joseph Flats half-graben and other regions to the west.

For much of its length, the Dry Wash fault is inferred to lie between the **jf** gravity and magnetic lows and the **NDWF** highs (figs. 10 and 11) that are adjacent to the southeast. Highs **NDWF** and its continuation, **DWF**, arc southwestward, continuing to approximately mark the southern boundary of the Clear Creek downwarp from where it passes under the Dry Wash fault, on the east, to within about 2 km of The Narrows, on the west. This suggests that the mapped en echelon monoclines in this region may be near-surface responses to displacement on a single deep-seated, north-side-down zone of displacement. The western edge of this downthrown block probably lies along the same north-northeast-trending normal faults that truncate the homoclines (TNFZ, fig. 6); they also truncate magnetic low **tn** (and its buried reversed-polarity flows?) on the west. Like the Joseph Flats block, this downthrown block may also contain low-density sediments, reflected by gravity low **tn** on figure 11. West of TNFZ, where the Clear Creek downwarp is expressed as a broad syncline, the magnetic signature is less-well defined, but may be reflected by an arcuate set of magnetic highs, **CCD** on figure 10. Highs **CCD** may reflect normal-polarity flows in the trough of the syncline, whose surfaces are sculpted by topography. Gravity features in this segment include a minor high (**CC** on fig. 11), but are poorly controlled by too-sparse gravity stations (map *B*). Furthermore, the southern part of the Pavant Range regional gravity gradient may obscure local subtle gravity signatures here.

Sevier fault zone and related fault trough

A deep structural and topographic trough between the northern Sevier Plateau and the Pavant Range enters the northeastern part of the map area (Sevier Valley, fig. 4). This trough extends south-southwest to opposite the trend of the Clear Creek downwarp, and then bends south, continuing to the southern edge of the map area. It is approximately bounded by the Sevier fault zone (fig. 6) on the east,

and by the Tushar fault, Dry Wash fault, Elsinore fault, and their extensions (fig. 6) on the west. Different segments of the trough show different gravity and magnetic configurations, and these will be described in sequence from north to south. The Marysvale Valley (fig. 4), between the Tushar and Marysvale Valley faults (fig. 6), is then discussed separately.

At its north end, between the Elsinore and Sevier faults (fig. 6), the trough is a well-defined graben having a significant thickness of alluvial fill. Abundant gravity stations define a deep low (about 25 mGal, **nsv**, fig. 11) that has sharp margins reflecting the graben's border faults. Assuming the density difference between horst rocks and graben fill is 0.3 g/cm^3, the Bouguer slab formula (fig. 12) predicts as much as 2,000 m of sediments there. Magnetic data show a broad, featureless low over most of the graben. Broad magnetic highs within the graben near its eastern boundary fault (the Sevier fault zone) may be due to magnetic sediments in alluvial fans at the mouths of streams draining the highlands to the east and southeast. This segment of the Sevier fault zone is clearly defined on the magnetic map by the western edge of a deep low on the Sevier Plateau (**tcl**, fig. 10). Surface geology over most of **tcl** consists of a jumble of small fault blocks that make up the Thompson Creek landslide. Low **tcl** probably reflects volcanic rocks having strong reversed remanent magnetization. The Three Creeks member of the Bullion Canyon Volcanics that crops out there has at least one subunit that was found by paleomagnetic measurements to be reversely polarized (the Wah Wah Springs Tuff of Caskey and Shuey, 1975). Some of the tuffs there were downslumped in the Thompson Creek landslide, but their consequent reorientations were probably limited to a few tens of degrees, not enough to greatly change their general (reversed) aeromagnetic signature. Additional reversed-polarity units may also be present at depth.

Farther south, where the northwest-dipping Dry Wash fault marks the western margin of a tilted intratrough fault block, the exposed low ridge of bedrock in the footwall of the fault is marked by a low linear gravity high (**NDWF**, fig. 11) and by a larger triangular-shaped magnetic high (**NDWF**, fig. 10). Magnetic high **NDWF** probably reflects volcanic sequences such as the Joe Lott Tuff Member (Tmj, table 2) that crop out in the low footwall ridge of bedrock and that are probably present beneath surficial alluvium in the valley to the east.

Rocks from nearby sources—Monroe Peak caldera to the east and Mount Belknap Volcanics to the west—affect the geophysical signature of the central part of the structural trough. The Monroe Peak caldera (fig. 6) has been traced westward across the eastern boundary fault (Sevier fault zone) nearly to the western margin of the structural trough in the central part of the map area (Cunningham and others, 1983; Rowley and others, 1986a,b, 1988a,b). Caldera rocks are widely exposed throughout this part of the trough, and many of the outcrops are at structural and stratigraphic levels comparable to those exposed in the eastern part of the caldera, high in the northern Sevier Plateau. Source intrusions of the Mount Belknap Volcanics (Tmi, table 2) also occupy some of the western part of the Monroe Peak caldera area. These relations suggest that density differences across the eastern margin of the fault trough should be minor. Nevertheless, the trend of the Sevier fault zone and the related trough west of it are quite clear on map *B*, for the whole western third of the caldera west of the fault zone is a broad gravity low (**csv**, fig. 11). This point is further discussed in the "Calderas" section, below.

The Sevier fault zone continues south from the Monroe Peak caldera area as a clearly defined topographic scarp. A narrow, linear magnetic low (**sfz**, fig. 10) marks part of this segment of the fault zone. The gravity low (labeled **ssv** for this portion of its length, fig. 11) continues from the north, following the structural trough, and reflecting alluvial fill in the valley between the fault zone and a medial bedrock ridge that is centered in the downfaulted trough for most of its length in the southern half of the map area.

Near the southern margin of the map area the regional fault trough is less sharply defined by gravity and magnetic data, although still quite apparent in the topography. The fault zones along the eastern and western margins are broader and more diffuse, and many slivers of bedrock cut by numerous dispersed faults crop out in the eastern half of the trough. The deepest part of the trough is near its western margin. These relationships are mirrored in the gravity configuration by a gravity ridge that correlates with the topographic ridge in the center of the trough (**ELB**, fig. 11), by the adjacent gravity low to the east (**elb**, fig. 11), and by an elongated gravity low that parallels the western margin of the trough and continues off the southern edge of the study area (**pr**, fig. 11).

The structural trough near the southern margin of the map area loses definition in the magnetic data within the area of dispersed faults. The magnetic birdseyes here reflect volcanic flows, with the highest

amplitude birdseyes (**ELB**, fig. 10) coinciding with basalt units.

Marysvale Valley block

A downfaulted block occupies the western part of the structural trough in the central part of the map area between the Tushar fault on the west and the Marysvale Valley fault on the east (fig. 6). This block is very deeply downfaulted at its southern end but only slightly so at its northern end. It is filled with a thick accumulation of fluvial and lacustrine deposits of the Miocene Sevier River Formation and with Quaternary alluvium. This alluvial fill depositionally onlaps the early to middle Miocene rhyolite lava flows of the Mount Belknap Volcanics exposed in the northern part of the basin. A deep gravity low (**mv**, fig. 11) clearly reflects this alluvial fill and suggests it is thickest in the southern two-thirds of the basin. Low **mv** is about 25 mGals deep. Assuming the density of sediments in the Marysvale Valley is some 2.00 g/cm^3 and that of surrounding rocks is about 2.40 g/cm^3, the Bouguer slab formula (fig. 12) predicts about 1,500 m of alluvial fill there. The magnetic configuration (map *A*) shows birdseyes over lava flows in the northern Marysvale Valley, but a relatively featureless low (**mv**, fig. 10) over the alluvium in the south, consistent with the expected signature of weakly magnetized alluvium.

Sulphurdale-Sheeprock fault zone

A complex zone of en echelon faults bounds the west side of the Tushar Mountains (fig. 4), just within the western margin of the map area (fig. 6). For the most part, these faults separate mountainous bedrock areas from alluviated valleys to the west. The contrast in densities is reflected by a linear gravity gradient along the trend of the Sulphurdale fault (**sul**, fig. 11). The eastern flanks of a basaltic andesite shield volcano centered just off the western margin of the map area give rise to the minor gravity high labeled **SV** (compare sample 79-S-44B). Near the north end of the Sulphurdale fault, bedrock is exposed on both sides of the fault and its gravity expression disappears. Alluvium-filled valleys are more prominent southward, where the gravity low west of the fault deepens.

The Sheeprock fault bounding the east side of Beaver Valley farther south is marked by a prominent, low topographic scarp along the west margin of the Tushar Mountains. Near the north end of the fault a gravity low (**bv**, fig. 11) marks an area of late Miocene rhyolite lava flows and alluvial valley fill in Beaver Valley (Evans and Steven, 1982). Farther south the mapped fault loses gravity expression, and a relative gravity high (**SBV**, fig. 11) extends out to the west-southwest over valley fill alluvium. This alluvial fill is cut by a braided series of Pleistocene-Holocene faults of small displacement (Machette and others, 1984) along **SBV**. These relations probably indicate that a shallow shelf of bedrock underlies thin valley fill just west of the Sheeprock fault and that a buried scarp farther west separates this shelf from thicker fill in the center of Beaver Valley. Note, though, that there are few gravity stations near the southern two-thirds of the Sheeprock fault to control the fields shown there.

Parts of the Sheeprock fault and, even more, the unnamed en echelon border fault south and southeast of it, have magnetic expression, with the exposed volcanic rocks in the footwall being expressed by a pattern of birdseye anomalies and the alluviated areas in the hanging wall by a broader and more simple pattern of anomalies. In particular, magnetic low **br** (fig. 10) falls over mafic volcanic rocks of Miocene age that cap Black Ridge (Tpm, table 2; sample M824, table 1); we infer these rocks to carry reversed magnetic polarity.

CALDERAS

The study area includes five calderas that formed in response to ash-flow eruptions (Steven, Rowley, and Cunningham, l984; figs. 5 and 6). From oldest to youngest, these are the Three Creeks caldera (about 27 Ma), Big John caldera (about 23 Ma), Monroe Peak caldera (about 23 Ma), Mount Belknap caldera (about 19 Ma), and Red Hills caldera (about 19 Ma; Steven, Rowley and Cunningham, 1984). Three of them are marked by subtle-to-strong gravity lows, whereas their magnetic expressions are variable.

Three Creeks caldera

The Three Creeks caldera in the northwestern part of the map area (Steven, l98l; fig. 6) underlies part of a local high on the relatively smooth gravity gradient of the Pavant Range, described above. A gravity terrace on a 1:250,000-scale regional gravity map (Cook and others, l98l) was interpreted by Steven, Rowley, and Cunningham (l984, fig. 9) to reflect a relatively dense source pluton at considerable depth whose more silicic cap had been expelled by the ash-flow eruptions that led to caldera collapse. The data on map *B* show this gravity

terrace as a crescentic concave-north high (**CC**, fig. 11) that is mostly outside the topographic wall of the caldera. Part of the gravity terrace may reflect the Clear Creek downwarp (above), and, at any rate, gravity stations in this area are too sparse to define its details. A similar configuration was described by Steven (l989) for the Crystal Peak caldera l00 km to the northwest, where a gravity anomaly associated with the caldera exceeds the dimensions of the subsided block and was interpreted to reflect a larger source magma chamber.

The Three Creeks caldera has no clear magnetic expression (map *A*). If there were a pluton below the caldera, we would expect it to have normal magnetic polarity, so as to give rise to a local magnetic high. No such magnetic high is seen, however. The magnetic signature of a large area north of the Clear Creek downwarp (**TC**, fig. 10), including the Three Creeks caldera area, consists of local magnetic highs that follow topographic highs and especially deep magnetic lows that follow topographic lows (compare figs. 4 and 10 to see this correlation). We interpret that the local magnetic highs must be due to normal-polarity flows of Bullion Canyon Volcanic rocks that are exposed at the surface and are sculpted by that topography. The extreme lows that fall over the deeper valleys incised into the Pavant Range argue that in these places the streams have cut away most of the normal-polarity rocks and have nearly exposed reversed-polarity units underneath.

Big John caldera

The Big John caldera, in the southwestern part of the study area, is a shallow trapdoor-type subsidence structure having a west-facing topographic wall along its eastern side (Steven, Cunningham, and Anderson, l984). A broad, shallow gravity trough (**bj**, fig. 11) extends north-northwest across the eastern part of the caldera, parallel to the topographic wall and in the general position of deepest subsidence. The western margin of the caldera is an obscure hingeline, and the flank of the gravity trough appears to be similarly diffuse in this direction. The gravity data do not indicate any specific intrusion occupying a source magma chamber, which Steven, Rowley, and Cunningham (l984) postulated to lie at relatively deep levels beneath the caldera area. Gravity stations there, however, are too sparse to make very reliable interpretations. Gravity low **bj** more clearly reflects the presence of the subsided basin and the younger, lighter fill within it; some of this fill includes relatively light rhyolitic welded ash-flow tuff of the Mount Belknap Volcanics. What was once the northern part of the Big John caldera is now obliterated by the younger Mount Belknap caldera. Gravity stations in that area are also too sparse to help resolve that boundary.

Magnetic anomalies in and near the Big John caldera are mostly low-amplitude birdseyes that make for a mottled green pattern on map *A*. Although there are moderately to highly altered rocks just outside the Big John caldera both to the east and west (fig. 5), rocks in the heart of the caldera are unaltered or only mildly (propylitically) altered (Cunningham, Steven, Rowley, and others, 1984). Exposures within the caldera are a complex mix of intermediate-composition lava flows (Tbc, table 2) and post-caldera rhyolite welded tuff (Tmj, table 2). Correlation between map *B* and the companion geologic map (Rowley and others, in press) shows that this subdued birdseye pattern generally reflects thicker sequences of Bullion Canyon Volcanics extrusive rocks. By contrast, Bullion Canyon Volcanics **intrusive** rocks lead to magnetic highs (features **BC**, discussed below), whereas thicker sequences of (unaltered) bimodal assemblage extrusive rocks (Mount Belknap Volcanics) lead to higher amplitude magnetic birdseyes.

Monroe Peak caldera

The Monroe Peak caldera occupies the east-central part of the study area. In general, the area of the caldera is marked by subtle gravity lows (**csv** and **mp**, fig. 11). As described by Steven, Rowley, and Cunningham (l984), the upper part of the caldera block consists of a cylinder of cogenetic intracaldera welded tuff more than 500 m thick; this tuff is widely altered, and its base has been invaded by numerous shallow plutons, some of which reached within 400 m or less of the surface. Post-subsidence lava flows derived from these shallow intrusions covered the floor of the caldera to local depths of as much as 400 m. The eastern two-thirds of the caldera is within the northern Sevier Plateau, one of the major topographic highs in this part of Utah. The Sevier fault zone along the west side of the plateau cuts across the caldera and exposes its core in cross section over a vertical distance of about l,500 m. The western one-third of the caldera exposes the upper part of the caldera fill at a structural and stratigraphic level only slightly below that exposed in the eastern part of the caldera. In addition, the western one-third of the caldera contains intrusive rocks of the younger Mount Belknap Volcanics (Tmi, table 2) and many irregular

patches of Mount Belknap Volcanics lava flows and welded tuffs. Younger alluvium is widely present in the western part of the caldera, but only locally is it more than a few tens of meters thick.

The eastern part of the caldera, in the Sevier Plateau, is marked by a broad gravity low. Geologic mapping based on generally good exposures shows that the northern margin of the caldera is nearly vertical and partly occupied by a postcaldera monzonitic intrusion. Relatively silicic intracaldera fill cut by a resurgent pluton is in steep contact with andesitic lava flows in the caldera wall. These lithologies, though contrasting, may represent rocks of similar densities (table 6), which might lead to minimal gravity change at the northern caldera wall; if anything, one might expect the monzonite intrusions inside the wall to lead to slightly higher gravity fields there. Observed gravity anomalies range from a high of about -190 mGal just north of the caldera wall to a low near -200 mGal one-quarter to one-third of the way into the caldera, to the south. There are enough gravity stations to demonstrate that this low exists, but they are too sparse to control its configuration closely. There may be a post-caldera pluton of higher density rock buried in the northern Sevier Plateau immediately north of, and perhaps extending under, the Monroe Peak caldera (**SP**, fig. 11); this could be the source pluton for the Oligocene-Miocene volcanic rocks of Signal Park.

The south wall of the Monroe Peak caldera in the Sevier Plateau area is fairly well defined by gravity data near the eastern edge of the study area, but toward the western edge of the plateau the gravity low extends southwest out of the area of the caldera (Cook and others, 1984). In this same area, advanced argillic alteration formed alunite deposits as much as l.2 km outside the topographic wall and perhaps as much as 2 km outside the structural wall of the caldera (Cunningham, Steven, Rowley, and others, l984). This alteration could have been related to an underlying postcaldera pluton, which also may be responsible for the gravity low.

The western one-third of the Monroe Peak caldera, west of the Sevier fault zone, is marked by an even deeper gravity low (**csv**, fig. 11) than that characterizing the caldera farther east. Although this area is nominally within a basin-and-range graben, caldera rocks are widely exposed. Here monzonite or other intrusions originally emplaced at depth in the Monroe Peak caldera have been juxtaposed east of the Sevier fault zone against rocks originally emplaced at higher levels west of it (Rowley and others, in press). The fault scarp here is some 1,500 m high, and the gravity change across it is about 12 mGal. The Bouguer slab formula (fig. 12) accordingly predicts a density difference of about 0.19 g/cm^3 between the juxtaposed rocks. Of samples collected from inside the caldera, monzonites from east of the fault (M569, M755, M914, and M915) all have densities close to 2.5 g/cm^3 , whereas samples collected west of the fault (M27A, M30, M47B, M49A, M50, M519, M522, M549, M608, M621, M713A, M713B, M851, M867, and M873) have widely varying densities. Five of these samples are altered and have densities in the range 1.617 to 2.162 g/cm^3. The rest fall into two groups: Monroe Peak caldera rocks, having densities in the range 2.520-2.736 g/cm^3, and two samples (M49A and M549) of later intrusive rocks of the Mount Belknap Volcanics series (Tmi, table 2), having densities of 2.319 and 2.291 g/cm^3, respectively. These latter two samples represent rocks from the eastern source area of the rhyolitic Mount Belknap Volcanics, which began intruding under the western one-third of the pre-existing Monroe Peak caldera about 21 Ma (Cunningham and Steven, 1979a; Cunningham, Unruh, and others, 1998). We interpret that gravity low **csv** reflects such source intrusions of the Mount Belknap Volcanics and rocks that were altered thereby. Present outcrops of unit Tmi probably represent cupolas on an extensive batholith or complex of stocks (Mount Belknap Volcanics were produced from this area from 21 Ma to 18 Ma, so that more than one stock under **csv** is likely (Cunningham and Steven, 1979a; Cunningham, Unruh and others, 1998). These intrusions may have a density of about 2.3 g/cm^3 and have an aggregate thickness of more than 1,400 m. Their eastern boundary may have localized the position of the later basin-and-range Sevier fault zone.

A great subcircular area of high magnetic values at least 35 km across occupies the central part of the northern Sevier Plateau (**CCP**, fig. 10), and is centered on and includes all of the Monroe Peak caldera. **CCP** clearly reflects rocks of high magnetization within the caldera, but it also extends several kilometers both north and south of the caldera, covering the mafic andesite volcanic center near Signal Peak to the north and the andesitic vent facies rocks of the Langdon Mountain volcanic center to the south.

The magnetic high that extends across the eastern Monroe Peak caldera (**CCP**, fig. 10) is subdued or absent west of the Sevier fault zone. To some extent, this may reflect the altered rocks present there (fig. 5). It could also reflect the above-inferred Mount

Belknap Volcanics source plutons under gravity low **csv** (fig. 11). The (unaltered) Monroe Peak caldera rock samples cited above have an average susceptibility of about 2.9×10^{-3} cgs, while the two cited samples of unit Tmi both had lower susceptibilities, 0.79×10^{-3} and 0.44×10^{-3} cgs. If Tmi rocks are pervasively present at depth, their relatively lower susceptibilities would explain the relatively lower observed aeromagnetic values west of the central part of the Sevier fault zone.

Mount Belknap caldera

The Mount Belknap caldera, in the west-central part of the study area, is marked by a 10-mGal bullseye gravity low centered in its southwest-central part (**mb**, fig. 11). The caldera outline is irregular, probably as a result of caving of unstable segments of the oversteepened wall during collapse of the caldera about l9 Ma. The actual subsided block is believed to be an oval about 8 × ll km across (Steven, Rowley, and Cunningham, l984), based in part on outcrops of wall rocks and in part on the gravity configuration. In particular, two outward projections of the caldera's topographic wall, to the north and to the east, are believed to have resulted from caving and to be underlain by inward-dipping walls that intersect the structural margin at depths of 2 km or less (Budding and others, l987). Cunningham and Steven (l979a) suggested that the underlying source magma chamber lay at shallow depths, with a top 3-4 km below the (then) surface. Gravity low **mb** probably reflects thick accumulations of rhyolites in the caldera. Assuming a density difference of 0.2 g/cm^3 between caldera rhyolite and underlying rocks, the Bouguer slab formula (fig. 12) predicts a thickness of about 1,200 m of rhyolite in the center of the Mount Belknap caldera.

An oval magnetic low (**smb**, fig. 10) parallels the south margin of the Mount Belknap caldera in the same area where vents for voluminous intracaldera rhyolite lava flows have been postulated (Cunningham and Steven, l979a). This low lies between, and nearly connects, two outcrops (Cunningham and others, 1983) of an intracaldera stock consisting of quartz latite (Tmic, table 2; sample M251). This stock cuts nearby rhyolite units, and its fluidal texture suggests that it was forcefully injected. Our interpretation is that the unit Tmic stock is present under low **smb**, that it is nonmagnetic relative to the surrounding rhyolitic flows, and that it represents a relatively local dike injected from a deeper parent magma up through a fairly thick pad of intracaldera rhyolites.

The aeromagnetic anomaly pattern in the south-central Mount Belknap caldera and in its eastern, shallower, lobe consists of low-amplitude birdseyes like those observed over the deeper parts of the Big John caldera. In both cases these magnetic patterns are thought to reflect varied alteration patterns in the intracaldera rhyolite. Most samples from these parts of the Mount Belknap caldera have low susceptibilities, but some (compare M206, M223) are less altered and have higher susceptibilities. A zone of altered rocks (fig. 5) was mapped (Cunningham, Steven, Rowley, and others, 1984; fig. 5) across the southern Mount Belknap caldera and outside it to the east. The mapped alteration zone does not extend south into the Big John caldera, but otherwise it generally corresponds to regions of subdued magnetic birdseyes on map *A*. Indeed, it may be possible to outline regions containing thick sequences of altered rocks by looking for this characteristic aeromagnetic pattern.

The magnetic pattern over the northern lobe of the Mount Belknap caldera also consists of birdseyes, but of higher amplitudes. Such a pattern typically characterizes volcanic flows. Caldera rocks in this area (compare sample M859) are unaltered. Also, precaldera wall rocks may underlie this part of the caldera at relatively shallow depths, locally adding to the magnetic complexity.

Red Hills caldera

The small Red Hills caldera along the western edge of the older Monroe Peak caldera is only about l.2 km across. A poorly controlled (by one station only) gravity low extends into the caldera from the Marysvale Valley low (**mv**, fig.11) to the south-southwest. Its magnetic signature consists of strong local highs on its east and west edges and broader lows on its north and south edges.

OTHER IGNEOUS FEATURES

Sulphurdale–Cove Fort area

The area northwest of the Mount Belknap caldera and east of the Sulphurdale fault is marked by a broad, extreme magnetic high (**S**, for "Sulphurdale high," fig. 10) and an equally broad, very deep low (**cf**, for "Cove Fort low," fig. 10) to the north. The transition between high and low makes a steep, east-trending magnetic gradient. It is remarkable that the most prominent high and the most prominent low in

the study area should be so juxtaposed, and the question arises whether they are related. In particular, could the Cove Fort low be a polarity effect of the Sulphurdale high?

The first answer to this question is that low **cf** is too broad and deep to be a **simple** polarity low from high **S**. This is shown by the fact that low **cf** is not substantially reduced by RTP processing (figs. 2 and 3). If both **S** and **cf** have a common source body, then that body is **not** magnetized along the direction of the Earth's present-day field, as we supposed for the RTP calculation.

The question then becomes whether **S** and **cf** could be polarity pairs from a common body that is magnetized in some other direction. Such a common source body would have to be large (some 15 km in diameter), and it would have to have high mafic mineral content so as to give rise to such a strong magnetization. If such a stock were present, it presumably would be part of the Pioche-Marysvale belt (fig. 1); hence, of Oligocene or Miocene age. Except in certain accreted terranes along the Pacific coast, western North American stocks of similar age commonly have paleomagnetizations of normal or reversed polarity, whereas near-zero (horizontal) paleomagnetic inclinations are rare. Furthermore, such large stocks cool slowly, giving rise to medium- or coarse-grained textures. Rocks that have such textures are prone to viscous remagnetization, so that their net magnetizations align with the present-day field direction, masking and replacing earlier components of magnetization in other directions. Paleomagnetic components in such rocks are minor, can be recovered only with painstaking work, and definitely are not observable on aeromagnetic maps. A stock that has a net nearly horizontal magnetization is therefore unlikely anywhere in western North America.

We conclude that the Sulphurdale high and Cove Fort low do not reflect a common source stock. **Separate** stocks under **S** and **cf** are still possible. According to the above argument, however, such stocks cannot maintain a reversed polarity. We therefore interpret that since low **cf** is not reduced by RTP processing, it must arise from reversed polarity flows, rather than a stock, in this area. We have inferred such flows to be present throughout the northern domain of the study area, causing lows **tcl**, **jf**, **tn**, and lows in area **TC**, as well as **cf**.

The Sulphurdale magnetic high (**S**, fig. 10) is interpreted to reflect a large pluton. Several pre-caldera monzonite intrusions that were emplaced shortly before 23 Ma (Tbci, table 2; samples M929, M930A,D) crop out in that area; these may coalesce into a single pluton at depth.

There are geothermal prospects near Cove Fort, and many solfataras and thermal springs nearby (Steven and Morris, 1983, 1986; Ross and others, 1982). These thermal features probably originate from a cooling pluton at depth, the likely magma source for Quaternary rhyolites and basalts that are west of the Sulphurdale fault. Gravity high **SV** (fig. 11) falls over one such Quaternary flow and may reflect this source pluton, as well. Because the pluton is still cooling, those parts of it that are now below Curie temperature should carry present-day (normal) magnetic polarity. We have not identified any aeromagnetic features that clearly relate to such a pluton, however.

Mill Creek–Red Narrows–Sevier Canyon area

Several interesting, still poorly understood, geological and geophysical features lie along and near the Mill Creek–Sevier Canyon streams (fig. 4) whose headwaters form along the northeast margin of the Mount Belknap caldera. An arcuate zone of faults (labeled NEMBC, fig. 6) roughly parallels the northeast margin of the Mount Belknap caldera. These faults may have formed in early Miocene time by resurgent uplift of a trapdoor block including the caldera. The NEMBC faults approximately bound on the northeast a gravity ridge (**K** and contiguous area to the south-southeast, fig. 11) that separates the Mount Belknap caldera gravity low, **mb**, from the extreme northwestern part of the Marysvale Valley low, **mv**. Gravity high **K** probably reflects the quartz monzonite pluton that crops out there (Tbci, table 2; samples M98, M177). Gold and silver produced during 1892–1937 in the Kimberly mining district (fig. 5) were mined from deposits near veins that cut this pluton. The gravity ridge extending south-southeast from **K** may reflect intermediate-composition volcanic rocks in the wall of the caldera that occur there in an upfaulted block. Sparse gravity stations in this area keep gravity high **K** and the gravity ridge to the south-southeast from being well controlled.

At Red Narrows (fig. 5) there is a deep, east-trending magnetic low (**rn**, fig. 10) whose source is unknown. Low **rn** extends east from the headwaters of Sevier Canyon for 10–12 km. As discussed above, **rn** is not an artifact of aeromagnetic data processing, for it appears on separate surveys flown in different

directions. Low **rn** has no explanation in surface geology, which consists of extensive sedimentary rocks of the Sevier River Formation, the underlying Joe Lott Member tuff (Tmj, table 2), and, at its eastern end, Quaternary landslide material. Low **rn** is deep enough to suggest a reversed-polarity unit at depth, perhaps the same as that which causes low **cf**. Lows **rn** and **cf** are separated, however, by an east-trending group of irregular highs under strip B; as discussed above, at least some of these highs persist despite probable misleveling of strip B. This pattern of local highs on background lows resembles that seen in area **TC** to the north, where that pattern reflects local topography. Here, though, such paleotopography, if present, is buried under ash-flow tuffs of unit Tmj. An alternative, less favored, explanation for anomaly **rn** is that it might reflect a swarm of east-trending, reversed-polarity dikes at this place. These dikes would have to be thin, so as to be quenched quickly enough to lock in the reversed polarity, and there would have to be a number of them to make up the observed width of anomaly **rn**. Such dikes, if present, could explain observed thermal and chamical anomalies at the Red Narrows clay-pits. Dike swarms, however, are not common in the Marysvale volcanic field. Whatever its cause, anomaly **rn** lies along, and helps define, the much longer east-striking Cove Fort transverse zone (figs. 2 and 3; Rowley and others, 1998).

Voluminous (150 km^3) ash-flow tuffs of the Joe Lott Tuff Member of the Mount Belknap Volcanics, unit Tmj, spewed northward from the Mount Belknap caldera at the time of its collapse, 19 Ma (Budding and others, 1987). The main channel for the early Joe Lott Member tuffs is speculated to have been near Mill Creek, north of Red Narrows (Budding and others, 1987), but later tuffs must have inundated much of the countryside. Remnants of unit Tmj occur north to about lat 38°30' N. over most the width of the study area, from near Cove Fort, on the west, to the Sevier Valley, on the east. Four subunits of unit Tmj have been recognized having a total measured stratigraphic thickness of 164 m (Budding and others, 1987). In much of the highlands north of Mount Belknap caldera and locally over the rest of its extent, unit Tmj is capped by sedimentary rocks of the Sevier River Formation.

Gravity low **sc** falls over Mill Creek and the headwaters of Sevier Canyon, and it may mark the paleotopographic channel followed by early tuffs of unit Tmj. Other parts of this channel are suggested by the northeast alignment of gravity lows **mb**, **sc**, **tn**, and possibly **jf**.

Sample M874 comes from Mill Creek, and has a density of 2.032 g/cm^3. Using this density together with the map *B* reduction density of 2.40 g/cm^3 in the Bouguer slab formula (fig. 12), we find about 300 m of material is needed to explain the 5-mGal low **sc**. Doing the same for low **tn**, and using a density of 1.71 g/cm^3 (sample M91), we find about 180 m of low-density material is needed to explain the >5-mGal low there. This is somewhat more than the total thickness of unit Tmj measured in the vicinity of the **tn** low. Both thicknesses, however, are not unreasonable values for depth of a paleovalley that could channel early ash-flow tuffs of unit Tmj. At any rate, the Bouguer slab formula (fig. 12) and the approximate values used with it are best used to constrain geologic scenarios and not to do precise analyses. Notice that the measured densities of these samples of unit Tmj decrease away from the source area, the Mount Belknap caldera, as they should for such ash-flow units.

Possible sources for aeromagnetic lows in the northern domain

Widespread ash-flow tuffs make excellent candidates for the reversed-polarity unit(s) that we postulate underlie much of the northern domain of the study area. Tuff units are quenched quickly, so that they can acquire and hold the magnetic direction that the Earth's field had at the time of their eruption. Ideally, because they have still higher mafic mineral content, basalts would be even better candidates for this role, but basalts are sparse in the Marysvale volcanic field relative to rhyolitic tuffs and, furthermore, their mode of extrusion is such that they might not blanket paleotopography as well as tuffs. The reversed-polarity unit(s) we are looking for must have covered a vast area, and they had to have blanketed that area thickly enough everywhere to leave no bare spots in the resulting magnetic low.

Caskey and Shuey (1975) made paleomagnetic measurements of many volcanic units of mostly Oligocene age in the Cove Fort–Sulphurdale area. Several units they measured had reversed polarity, among them the Wales Canyon Tuff (Tw on the companion map by Rowley and others, in press; not listed in table 2; no samples), the Wah Wah Springs Formation (Tnw on the companion map of Rowley and others, in press), and several other tuffs formerly correlated with the Needles Range Group (Tn, table 2). The Wales Canyon Tuff has a thickness of 60 m (Caskey and Shuey, 1975) at the place where it crops

out, a strip underlying magnetic low **wc** (fig. 10), and it strikes north-northeast for a total distance of about 8 km. Unit Tw could underlie much of the southwestern Pavant Range at depth, so as to cause the northern-domain magnetic low, but the aeromagnetic low, **wc**, over its outcrop is not impressive. Some other (deeper?) unit is probably responsible, but it remains unidentified. A possible candidate is a unit or units formerly correlated with the Needles Range Group (see Tn, table 2) but now largely correlated with the Three Creeks Tuff Member of the Bullion Canyon Volcanics (Tbct, table 2), which crop out in several places in the northern domain of the study area and which may underlie much of the rest of it. Recall that we have interpreted the local lows interspersed with highs in area **TC** (fig. 10) to reflect reversed polarity units that may crop out in canyons or be shallowly buried there. Many such lows do correlate with the Three Creeks Member of the Bullion Canyon Volcanics (Tbct, table 2), so we interpret that at least some (deeper?) subunits of unit Tcbt carry strong reversed polarity. Note, though, that at least one sample of unit Tbct (M908, table 1) showed normal polarity in a field test. Because many relative highs in area **TC** correlate with rocks of the Bullion Canyon Volcanics (Tbc, table 2) that locally overlie unit Tbct, we also interpret that these local rocks of unit Tbc carry normal polarity.

Area **TC** falls over a block that is faulted up relative to blocks to the southeast (across TNFZ, fig. 6) and southwest (across the Cove Fort fault and other faults splaying from it, fig. 6). These nearby blocks also display deep aeromagnetic lows (**jh** and **cf**, fig. 10), so they too must contain reversed-polarity units. The northeastern part of **jh** (fig. 10) correlates with basaltic andesites (Ta, table 2) that cover the slopes of hills of the Pavant Range just northwest of Joseph Flats (fig. 4). Low **jh** extends far to the southwest, however, over an upthrown block largely capped by Joe Lott Tuff Member (Tmj, table 2). Elsewhere, at Red Narrows (fig. 4), unit Tmj appears to be normally polarized (see above discussion of aeromagnetic low **rn**). This normally polarized magnetization is probably weak, though, for measured samples (M91, M92, M809) of unit Tmj have relatively low susceptibility and NRM values. Therefore, the southwestern extension of low **jh** may reflect a reversed-polarity unit buried under unit Tmj.

There are no geologic units that clearly correlate with low **cf**. Finding the source rocks for low **cf**, therefore, remains an unsolved puzzle in interpretating map *A*. Such source rocks must be buried, and they must be extensive at depth. A difficulty with ascribing northern-domain lows to any buried unit is that, in this study area, the units that overlie it may carry normal polarity. The fields of any such overlying normal-polarity units will oppose those of the buried reversed-polarity unit. The deeper the proposed source unit, the thicker it must be and the stronger its reversed-polarity NRM must be to explain the northern-domain low. Note, though, that more than one reversed-polarity unit may be responsible for the lows.

Mount Holly–Bellyache Canyon low

Aeromagnetic low **rn** has an interesting counterpart to the south in low **mhbc**, fig. 10. Low **mhbc** is a deep low or series of lows that extends from Mount Holly ski area in the Big John caldera, on the west, to Bellyache Canyon, draining into southern Marysvale Valley, on the east. The principal exposed geologic units in the area of low **mhbc** are three subunits of the Bullion Canyon Volcanics; the Upper Member (Tbu, table 2; samples M263, M903, and M905), the Middle Member (Tbm, table 2; sample M261), and the Delano Peak Tuff Member (Tbcd, table 2; sample M902). As was the case with low **rn**, the exposed units under low **mhbc** are areally extensive, and their boundaries do not correlate with the edges of the aeromagnetic feature. For that reason, and because Bullion Canyon Volcanics in other parts of the study area have a different aeromagnetic signature (subdued birdseyes), we think it unlikely that they are the source rocks for **mhbc**. The eastern end of **mhbc** occurs over volcanic rocks of the Mount Dutton Formation (Td, table 2; samples M468, M470, and 78-698), and several local lows extending south from it also fall over either unit Td or surficial alluvium that probably covers unit Td. Therefore, we interpret that low **mhbc** is due to buried parts of unit Td that have reversed magnetic polarity. Source vents for the upper Oligocene–lower Miocene Mount Dutton Formation are thought to lie to the south of here (Rowley and others, 1994). As is the case for **rn**, we further interpret that these source flows may have pooled in a topographic low. Our tentative picture, therefore, is that by late Oligocene– early Miocene time, the central part of the ancestral Marysvale volcanic field contained at least two deep east-trending canyons, in which there accumulated deposits of tuffs of the Needles Range Group and the Three Creeks Tuff Member of the Bullion Canyon Volcanics, coming from the north, and lava flows and

mud flows of Mount Dutton Formation, coming from the south. This east-trending feature may be related to the Blue Ribbon transverse zone, located farther to the south (fig 2; Rowley and others, 1998; Rowley, 1998).

Selected local plutons

Many other aeromagnetic features on map *A* remain to be interpreted. Some of these are local highs that are wider than the birdseyes due to volcanic rocks and that probably reflect either plutons or volcanic units such as basalt flows or tuffs. In many places, the probable source rocks crop out and can be identified by correlating the features on map *A* with geologic units on the companion geologic map of Rowley and others (in press) or on the 1:50,000-scale map of Cunningham and others (1983). Examples include highs **LJ** (fig. 10) and the Formation of Lousy Jim (Sigmund, 1979; Tlj, table 2; sample M505); high **B** (fig. 10) and Tertiary basalts (Tbas, table 2; sample M801); highs **BC** and **Y** (fig. 10) and Bullion Canyon Volcanic intrusive (Tbci, table 2: no nearby samples) and, to a lesser extent, extrusive (Tbc, table 2) rocks. High **Y** is particularly noteworthy because it may reflect a pluton responsible for the 14-Ma Rhyolite of Big Star (Cunningham and others, 1983) and associated natroalunite deposits north of the Red Hills caldera.

One particular use of detailed aeromagnetic maps such as map *A* is to identify reentrant lows into broader highs, for these can reflect altered parts of plutons that may be significant in exploring for base and precious metals. An example from this study area is the Indian Peaks high (**IP**, fig. 10) and associated Mystery Sniffer mine (fig. 5), discussed by Cunningham, Steven, Campbell, and others (1984).

SUMMARY AND CONCLUSIONS

Density and magnetic properties were measured for 88 samples of igneous rocks from the Marysvale volcanic field. Dry bulk density, magnetic susceptibility, and NRM generally decrease as the degree of alteration increases, reflecting increases in content of hydrated low-density minerals, increases in porosity, and decreases in magnetite content. This implies that larger volumes of altered rock may show up as lows on both gravity (map *B*) and aeromagnetic maps (map *A*). An exception, important in the Marysvale volcanic field because of the kind of altered rock present, is the increase in density when alteration has proceeded to the extent that alunite is formed (for example, sample M53). Gravity stations in the Marysvale volcanic field are too sparse to be able to pick out medium- to small-sized, alunite-altered areas on a gravity map, however. Hematite is the stable iron-oxide mineral in the acid sulfate environment that leads to the formation of alunite; consequently, the magnetic susceptibility and NRM of alunite-altered rocks, like those of most other altered rocks, are low.

The densest rocks in the Marysvale volcanic field are basalts having typical bulk densities of about 2.6 g/cm^3; these rocks also have the highest typical magnetic susceptibility (20×10^{-4} cgs) and NRM (45×10^{-4} emu/cm^3). Typical values of density, magnetic susceptibility and NRM increase with mafic index for both extrusive and intrusive rock samples from the Marysvale volcanic field. Rocks of the Bullion Canyon Volcanics have typical values of these three properties that are somewhat higher than corresponding values for rocks of the Mount Belknap Volcanics. This reflects the changeover from earlier rocks of intermediate composition (Bullion Canyon Volcanics) to later alkali rhyolite rocks of the bimodal suite (Mount Belknap Volcanics).

No such systematic variations were seen in measured values of Koenigsberger Q ratios. Typical unaltered igneous rocks from the Marysvale volcanic field have high values of Q, however; so that their permanent magnetization (NRM) components outweigh their induced magnetization (susceptibility) components. This in turn implies that the aeromagnetic fields seen on map *A* result principally from NRM. Therefore, volcanic flows that were extruded during reversed-polarity epochs may carry reversed magnetizations, and, hence, appear as deep lows on aeromagnetic maps. For plutons, however, it is likely that the observed NRM principally reflects a viscous magnetization component that is now aligned with the present Earth's field, so that plutons should carry normal magnetization and appear as highs on map *A*.

The Pioche-Marysvale igneous belt shows up on the regional magnetic map as a belt of magnetic highs flanked to the north and (in places) south by magnetic lows. Some of these lows are dispersed by RTP processing, a technique that reduces polarity lows and moves magnetic signatures more directly over their source bodies. The lows in the northern part of the study area remain, however, implying that these lows are due to sources with reversed magnetization.

The study area can be divided into three geophysical domains on the basis of their gravity and

aeromagnetic signatures. The northern domain has a strong gravity gradient decreasing to the south and low or very low aeromagnetic fields. The central domain has low gravity fields and moderate aeromagnetic fields including several large highs. The southern domain has intermediate gravity fields and birdseye (high spatial-frequency highs and lows) magnetic fields. A deep, south-trending gravity low along the Sevier and Marysvale Valleys cuts all three domains, reflecting through-going basin-and-range graben(s).

Aeromagnetic lows in the northern domain are interpreted to reflect sequences of reversed-polarity tuffs that may include units of the late Oligocene–early Miocene Three Creeks Member of the Bullion Canyon Volcanics. As these tuffs spread to the south they may have accumulated in a paleo-valley located at the boundary between northern and central domains. There are no aeromagnetic features that can be interpreted to reflect plutons in the northern domain of the study area. The gravity gradient in the northern domain probably reflects the southern flank of a regional structural dome centered north of the study area. This dome, the Sevier River oval (T.A. Steven, written commun., 1985) may represent a mantle upwarp of basin-and-range and older age (Thompson and Zoback, 1979). As the dome pushed up, the overlying volcanic units were stretched and faulted in ways that are reflected on the aeromagnetic map.

The central domain marks the eruptive center of the Marysvale volcanic field. Its northern boundary is the Cove Fort transverse zone, and its southern boundary is the Blue Ribbon transverse zone (Rowley and others, 1998; Rowley, 1998). The general gravity low there probably reflects the lower densities of these igneous intrusions, whereas the general aeromagnetic high of the central domain reflects their normal-polarity (viscous) NRM. Particular magnetic highs may mark particular intrusion complexes south of Sulphurdale, north of the Red Hills caldera, and under the central Sevier Plateau, among others. Deep gravity lows associated with the Big John and Mount Belknap calderas reflect accumulations of relatively light rhyolitic volcanic rocks that have accumulated therein. The central domain contains many areas of altered rocks, and the hydrothermal processes that gave rise to this alteration also emplaced base- and precious-metal deposits in the domain. Areas of altered rocks contribute to gravity lows in calderas and show up on the aeromagnetic map as reentrant lows into highs that reflect plutons. Such reentrant lows can help locate subsequent, sometimes porphyritic, intrusions into an earlier pluton. Where the rocks are of the bimodal assemblage, altered zones can show up as areas of attenuated birdseyes on the aeromagnetic map. Such attenuated birdseyes typically appear as mottled shades of green on map *A*, and are evident in the Kimberly and Central Mining Areas (fig. 5). This generalization is clouded, however, because **unaltered** Bullion Canyon Volcanics extrusive rocks also have this attenuated birdseye signature.

The southern domain is characterized by high-amplitude birdseyes that reflect tuffs and mafic lava flows and mudflow breccias. Deeper lows may reflect reversed-polarity volcanics, possibly of the Mount Dutton Formation. We interpret that at least one such reversed-polarity unit may have onlapped from the south to collect in a paleovalley located along the boundary between central and southern domains. There are no large aeromagnetic highs that we can ascribe to plutons in the southern domain of the study area.

Calderas in the study area have variable gravity and aeromagnetic signatures that reflect their different sizes and characters. The Red Hills caldera is so small that no clear gravity or aeromagnetic signature can be ascribed definitely to it. The Three Creeks caldera may give rise to a subtle gravity high. Its aeromagnetic signature, if any, has now been masked by later reversed- and normal-polarity flows that blanketed the area. Gravity lows reflecting low-density intracaldera flows, and low-amplitude birdseye aeromagnetic patterns reflecting the varied compositions and alteration patterns of these intracaldera flows, are associated with both Big John and Mount Belknap calderas. Because the Mount Belknap caldera was a deep caldron, whereas the Big John caldera was a shallow trapdoor subsidence structure, the gravity low over the Mount Belknap caldera is relatively deeper. Magnetic highs in the eastern part of the Monroe Peak caldera apparently reflect local plutons. The deep gravity low in its western one-third probably reflects a complex of post-caldera intrusions that were the eastern source zone for the Mount Belknap Volcanics. All five calderas in the study area evidently were small enough to be supported in large part by the local crust, for they do not show the gravity highs that characterize resurgent domes that have isostatically rebounded.

ACKNOWLEDGMENTS

We thank the USGS Paleomagnetism Laboratory, Denver, Colo., for use of their facilities, Rob Meyer for measuring susceptibility and remanance of our rock samples, and Tien Grauch and Viki Bankey for careful reviews of the manuscript.

REFERENCES CITED

Anderson, J.J., Rowley, P.D., Blackman, J.T., Mehnert, H.H., and Grant, T.C., 1990a, Geologic map of the Circleville Canyon area, southern Tushar Mountains and northern Markagunt Plateau, Beaver, Garfield, Iron, and Piute Counties, Utah: U.S. Geological Survey Miscellaneous Investigations Series Map I-2000, scale 1:50,000.

Anderson, J.J, Rowley, P.D., Machette, M.N., Decatur, S.H., and Mehnert, H.H., 1990b, Geologic map of the Nevershine Hollow area, eastern Black Mountains, southern Tushar Mountains, and northern Markagunt Plateau, Beaver and Iron Counties, Utah: U.S. Geological Survey Miscellaneous Investigations Series Map I-1999, scale 1:50,000.

Anderson, R.E., and Barnhard, T.P., 1992, Neotectonic framework of the central sevier Valley area, Utah, and its relationship to seismicity, *in* Gori, P.L., and Hays, W.W., eds., Assessment of regional earthquake hazards and risk along the Wasach front, Utah: U.S. Geological Survey Professional Paper 1500-K, 47 p.

Bath, G.D., 1968, Aeromagnetic anomalies related to remanent magnetism in volcanic rock, Nevada Test Site, *in* Eckel, E.B., ed., Nevada Test Site: Geological Society of America Memoir 110, p. 135-146.

Beaty, D.W., Cunningham, C.G., Rye, R.O., Steven, T.A., and Gonzalez-Urien, E., 1986, Geology and geochemistry of the Deer Trail Pb-Zn-Ag-Au-Cu manto deposits, Marysvale District, west-central Utah: Economic Geology, v. 81, no. 8, p. 1932-1952.

Best, M.G.,and Grant, S.K., 1987, Stratigraphy of the volcanic Needles Range Group in southwestern Utah: U.S. Geological Survey Professional Paper 1433-A, 28 p.

Best, M.G., McKee, G.H., and Damon, P.E., 1980, Space-time-composition patterns of late Cenozoic mafic volcanism, southwestern Utah and adjoining areas: American Journal of Science, v. 280, p. 1035-1050.

Blakely, R.J., 1994, Potential theory in gravity and magnetic applications: New York, N.Y., Cambridge University Press, p. 330-342.

Budding, K.E., Cunningham, C.G., Zielinski, R.A., Steven, T.A., and Stern, C.R., 1987, Petrology and chemistry of the Joe Lott Tuff Member of the Mount Belknap Volcanics, Marysvale volcanic field, west-central Utah: U.S. Geological Survey Professional Paper 1354, 47 p.

Campbell, D.L., Cunningham, C.G., Steven, T.A., Rowley, P.D., Glassgold, L.B., and Anderson, J.J., 1984, Aeromagnetic and geologic map of the Tushar Mountains and adjoining areas, Marysvale volcanic field, Utah: U.S. Geological Survey Miscellaneous Investigations Series Map I-1430-D, scale 1:50,000.

Campbell, D.L., and Flanigan, V.J., 1982, Geophysical measurements in the Beaver Basin, west-central Utah; Part 2 — Resistivity, IP, and seismic investigations: U.S. Geological Survey Open-File Report 82-420, 44 p.

Caskey, C.F., and Shuey, R.T., 1975, Mid-Tertiary volcanic stratigraphy, Sevier–Cove Fort area, central Utah: Utah Geology, v. 2, no. 1, p. 17-25.

Cook, K.L., Adhidjaja, J.I., and Gabbert, S.C., 1981, Complete Bouguer gravity anomaly and generalized geology map of Richfield $1^\circ \times 2^\circ$ quadrangle, Utah: State of Utah Department of Natural Resources and Energy, Utah Geological and Mineral Survey, Map 59, scale 1:250,000.

Cook, K.L., Bankey, Viki, Mabey, D.R., and DePangher, M., 1989, Complete Bouguer gravity anomaly map of Utah: State of Utah Department of Natural Resources and Energy, Utah Geological and Mineral Survey, Map 122, 1 sheet, scale 1:500,000.

Cook, K.L., Halliday, M.E., Cunningham, C.G., Steven, T.A., Rowley, P.D., Glassgold, L.B., Anderson, J.J., and Coles, L.L., 1984, Complete Bouguer gravity anomaly and geologic map of the Tushar Mountains and adjoining areas, Marysvale volcanic field, Utah: U.S. Geological Survey Miscellaneous Investigations Series Map I-1430-C, scale 1:50,000.

Cook, K.L., Montgomery, J.R., Smith, J.R., and Gray, E.G., 1975, Simple Bouguer gravity anomaly map of Utah: State of Utah Department of Natural Resources and Energy, Utah Geological and Mineral Survey, Map 37, scale 1:1,000,000.

Cook, K.L., Serpa, L.F., and Pe, W., 1980, Detailed

gravity and aeromagnetic surveys of the Cove Fort Sulphurdale KGRA and vicinity, Millard and Beaver counties, Utah: University of Utah, Department of Geology and Geophysics, Topical Report DOE/ET/2839230, DOE/DGE Contract AC07-78ET28392, 88 p.

Cunningham, C.G., Rasmussen, J.D., Steven, T.A., Rye, R.O., Rowley, P.D., Romberger, S.B., and Selverstone, J., 1998, Hydrothermal uranium deposits containing molybdenum and fluorite in the Marysvale volcanic field, west-central Utah: Mineralium Deposita, v. 33, no. 4, p. 447-494.

Cunningham, C.G., Rye, R.O., Bethke, P.M., and Logan, M.A.V., 1997, Vein alunite formed by episodic degassing of an epizonal stock [abs.]: Eos, American Geophysical Union, v. 78, no. 46, p. F746.

Cunningham, C.G., Rye, R.O., Steven, T.A., and Mehnert, H.H., 1984, Origins and exploration significance of replacement and vein-type alunite deposits in the Marysvale volcanic field, west-central Utah: Economic Geology, v. 79, no. 1, p. 50-71.

Cunningham, C.G., and Steven, T.A., 1979a, Mount Belknap and Red Hills calderas and associated rocks, Marysvale volcanic field, west-central Utah: U.S. Geological Survey Bulletin 1468, 34 p.

Cunningham, C.G., and Steven, T.A., 1979b, Environments favorable for the occurrence of uranium within the Mount Belknap caldera, Beaver Valley and Sevier River Valley, west-central Utah: U.S. Geological Survey Open-File Report 79-434, 15 p.

Cunningham, C.G., and Steven, T.A., 1979c, Uranium in the Central Mining Area, Marysvale district, west-central Utah: U.S. Geological Survey Miscellaneous Investigations Series Map I-1177, scale 1:24,000.

Cunningham, C.G., and Steven, T.A., 1979d, Geologic map of the Deer Trail Mountain–Alunite Ridge mining area, west-central Utah: U.S. Geological Survey Miscellaneous Investigations Series Map I-1230, scale 1:24,000.

Cunningham, C.G., Steven, T.A., Campbell, D.L., Naeser, C.W., Pitkin, J.A., and Duval, J.S., 1984, Multiple episodes of igneous activity, mineralization, and alteration in the western Tushar Mountains, Utah: U.S. Geological Survey Professional Paper 1299-A, 21 p.

Cunningham, C.G., Steven, T.A., Rowley, P.D., Glassgold, L.B., and Anderson, J.J., 1983, Geologic map of the Tushar Mountains and adjoining areas, Marysvale volcanic field, Utah: U.S. Geological Survey Miscellaneous Investigations Series Map I-1430-A, scale 1:50,000.

Cunningham, C.G., Steven, T.A., Rowley, P.D., Glassgold, L.B., and Anderson, J.J., 1984, Map of argillic and advanced argillic alteration and principal hydrothermal quartz and alunite veins in the Tushar Mountains and adjoining areas, Marysvale volcanic field, Utah: U.S. Geological Survey Miscellaneous Investigations Series Map I-1430-B, scale 1:50,000.

Cunningham, C.G., Steven, T.A., Rowley, P.D., Naeser, C.W., Mehnert, H.H., Hedge, C.E., and Ludwig, K.R., 1994, Evolution of volcanic rocks and associated ore deposits in the Marysvale volcanic field, Utah: Economic Geology, v. 89, p. 2003-2005.

Cunningham, C.G., Unruh, D.M., Steven, T.A., Rowley, P.D., Naeser, C.W., Mehnert, H.H., Hedge, C.E., and Ludwig, K.R., 1998, Geochemistry of volcanic rocks in the Marysvale volcanic field, west-central Utah, *in* Friedman, J.D., and Huffman, A.C., Jr., eds., Laccolith complexes of southeastern Utah: Time of emplacement and tectonic setting–Workshop proceedings: U.S. Geological Survey Bulletin 2158, p. 223-232.

Earth Sciences Laboratory, 1978, Residual aeromagnetic map, Cove Fort–Sulphurdale, Dog Valley areas, Utah: Salt Lake City, Utah, University of Utah Research Institute, Open-File Data UT/CFS/ESL-1, scale 1:62,500.

Evans, S.H., Jr., and Steven, T.A., 1982, Rhyolites in the Gillies Hill–Woodtick Hill area, Beaver County, Utah: Geolological society of America Bulletin, v. 93, no. 11, p. 1131-1141.

Flanigan, V.J., and Campbell, D.L., 1981, Geophysical studies in the Beaver Basin, west-central Utah; Part 1 — Slingram, magnetic, and spontaneous polarization profiles: U.S. Geological Survey Open-File Report 81-199, 5 p., 11 figs.

Geological Society of America, 1984, Decade of North American Geology Geologic Time Scale: Geological Society of America Map and Chart Series MC-50.

Halliday, M.E., and Cook, K.L., 1980, Regional gravity survey, northern Marysvale volcanic field, south-central Utah: Geological Society of America Bulletin, Part I, v. 91, p. 502-508.

Jachens, R.C, and Moring, B.C., 1990, Maps of the thickness of Cenozoic deposits and the isostatic residual gravity over basement for Nevada: U.S. Geological Survey Open-file Report 90-404, 15 p.

Johnson, G.R., 1979, Textural properties: U.S. Geological Survey Circular 789, p. 67-74.

Machette, M.N., Steven, T.A., Cunningham, C.G., and Anderson, J.J., 1984, Geologic map of the Beaver quadrangle, Beaver and Piute Counties, Utah: U.S. Geological Survey Miscellaneous Investigations Series Map I-1520, scale 1:50,000.

Mackie, R.L., and Cunningham, C.G., 1982, Density and magnetic susceptibility measurements of igneous rocks from the Marysvale volcanic field, west-central Utah: U.S. Geological Survey Open-File Report 82-892, 25 p.

Miller, W.R., Motooka, J.M., Cunningham, C.G., Steven, T.A., Rowley, P.D., and Anderson, J.J., 1984a, Distribution of anomalous trace elements in the nonmagnetic fraction of heavy-mineral concentrates of stream sediments, shown on a geologic base map of the Tushar Mountains and adjoining areas, Marysvale volcanic field, Utah: U.S. Geological Survey Miscellaneous Investigations Series Map I-1430-E, scale 1:50,000.

Miller, W.R., Motooka, J.M., Cunningham, C.G., Steven, T.A., Rowley, P.D., and Anderson, J.J., 1984b, Distribution of anomalous trace elements in the magnetic fraction of heavy-mineral concentrates of stream sediment, shown on a geologic base map of the Tushar Mountains and adjoining areas, Marysvale volcanic field, Utah: U.S. Geological Survey Miscellaneous Investigations Series Map I-1430-F, scale 1:50,000.

Miller, W.R., Motooka, J.M., Cunningham, C.G., Steven, T.A., Rowley, P.D., and Anderson, J.J., 1984c, Distribution of anomalous trace elements in the less-than-180-micrometer fraction of stream sediments, shown on a geologic base map of the Tushar Mountains and adjoining areas, Marysvale volcanic field, Utah: U.S. Geological Survey Miscellaneous Investigations Series Map I-1430-G, scale 1:50,000.

Plouff, Donald, and Pakiser, L.C., 1972, Gravity study of the San Juan Mountains, Colorado: U.S. Geological Survey Professional Paper 800-B, p. B183-B190.

Ross, H.P., Moore, J.N., and Christensen, O.D., 1982, The Cove Fort–Sulfurdale KGRA, a geologic and geophysical case study: Salt Lake City, Utah Earth Sciences Laboratory, University of Utah Research Institute.

Rowley, P.D., 1998, Cenozoic transverse zones and igneous belts in the Great Basin, western United States—Their tectonic and economic implications, *in* Faulds, J.E., and Stewart, J.H., eds., Accomodation zones and transfer zones: the regional segmentation of the Basin and Range province: Geological Society of America Special Paper 323, 266 p.

Rowley, P.D., Cunningham, C.G., Steven, T.A., Mehnert, H.H., and Naeser, C.W., 1988a, Geologic map of the Marysvale quadrangle, Piute County, Utah: Utah Geological and Mineral Survey Map 105, scale 1:24,000; includes 15-p. drop-in pamphlet.

Rowley, P.D., Cunningham, C.G., Steven, T.A., Mehnert, H.H., and Naeser, C.W., 1988b, Geologic map of the Antelope Range quadrangle, Sevier and Piute Counties, Utah: Utah Geological and Mineral Survey Map 106, scale 1:24,000; includes 14-p. drop-in pamphlet.

Rowley, P.D., Cunningham, C.G., Steven, T.A., Mehnert, H.H., and Naeser, C.W., 1998, Cenozoic igneous and tectonic setting of the Marysvale volcanic field and its relation to other igneous centers in Utah and Nevada, *in* Friedman, J.D., and Huffman, A.C., Jr., eds. Lacolith complexes of southeastern Utah: time of emplacement and tectonic setting — Workshop proceedings: U.S. Geological Survey Bulletin 2158, p. 167-201.

Rowley, P.D., Cunningham, C.G., Steven, T.A., Workman, J.B., Anderson, J.J., and Theissen, K.M, in press, Geologic map of the central Marysvale volcanic field, southwestern Utah: U.S. Geological Survey Geologic Investigations Series I-2645-A, scale 1:100,000.

Rowley, P.D., Hereford, Richard, and Williams, 1987, Geologic map of the Adams Head–Johns Valley area, southern Sevier Plateau, Garfield County, Utah: U.S. Geological Survey Miscellaneous Investigations Series Map I-1798, scale 1:50,000.

Rowley, P.D., Mehnert, H.H., Naeser, C.W., Snee, L.W., Cunningham, C.G., Steven, T.A., Anderson, J.J., Sable, E.G., and Anderson, R.E., 1994, Isotopic ages and stratigraphy of Cenozoic rocks of the Marysvale volcanic field and adjacent areas, west-central Utah: U.S. Geological Survey Bulletin 2071, 35 p.

Rowley, P.D., Steven, T.A., Anderson, J.J., and

Cunningham, C.G., 1979, Cenozoic stratigraphy and structural framework of southwestern Utah: U.S. Geological Survey Professional Paper 1149, 22 p.

Rowley, P.D., Steven, T.A., and Mehnert, H.H., 1981, Origin and structural implications of upper Miocene rhyolites in Kingston Canyon, Piute County, Utah: Geological Society of America Bulletin, Part I, v. 92, p. 590-602.

Rowley, P.D., Williams, P.L., and Kaplan, A.M., 1986a, Geologic map of the Greenwich quadrangle, Piute County, Utah: U.S. Geological Survey Geologic Quadrangle Map GQ-1589, scale 1:24,000.

Rowley, P.D., Williams, P.L., and Kaplan, A.M., 1986b, Geologic map of the Koosharem quadrangle, Sevier and Piute Counties, Utah: U.S. Geological Survey Geologic Quadrangle Map GQ-1590, scale 1:24,000.

Saltus, R.W., and Jachens, R.C., 1995, Gravity and basin-depth maps of the Basin and Range Province, Western United States: U.S. Geological Survey Geophysical Investigations Map GP-1012, scale 1:2,500,000.

Schutter, T.A., Duval, J.S., Campbell, D.L., Pitkin, J.A., Steven, T.A., Cunningham, C.G., 1989, Gamma-ray composite-color maps of the Tushar Mountains and adjoining areas, Marysvale volcanic field, Utah: U.S. Geological Survey Miscellaneous Investigations Series Map I-1430-H, scale 1:100,000; 4 maps with text.

Sigmund, J.M., 1979, Geology of a Miocene rhyodacite lava flow, southern Tushar Mountains: Kent, Ohio, Kent State University, M.S. thesis, 35 p.

Spiegel, M.R., 1961, Theory and Problems of Statistics: New York, McGraw-Hill Book Company, Schaum's Outline Series, 359 p.

Steven, T.A., 1981, Three Creeks caldera, southern Pavant Range, Utah: Brigham Young University Geology Studies, v. 28, pt. 3, p. 1-7.

Steven, T.A., 1984, ed., Igneous activity and related ore deposits in the western and southern Tushar Mountains, Marysvale volcanic field, west-central Utah: U.S. Geological Survey Professional paper 1299-A,B, 33 p.

Steven, T.A., 1989, Geologic map of the Crystal Peak caldera, west-central Utah: U.S. Geological Survey Miscellaneous Investigation Series Map I-2002, scale 1:100,000.

Steven, T.A., Cunningham, C.G., and Anderson, J.J., 1984, Geologic history and uranium potential of the Big John caldera, southern Tushar Mountains, Utah, *in* Steven, T.A., ed., Igneous activity and related ore deposits in the western and southern Tushar Mountains, Marysvale volcanic field, west-central Utah: U.S. Geological Survey Professional Paper 1299-B, p. 23-33.

Steven, T.A., Cunningham, C.G., and Machette, M.N., 1981, Integrated uranium systems in the Marysvale volcanic field, west-central Utah, *in* Goodell, P.C., and Waters, A.C., eds., Uranium in volcanic and volcaniclastic rocks: American Association of Petroleum Geologists Studies in Geology, no. 13, p. 111-122.

Steven, T.A., Cunningham, C.G., Naeser, C.W., and Mehnert, H.H., 1979, Revised stratigraphy and radiometric ages of volcanic rocks and mineral deposits in the Marysvale area, west-central Utah: U.S. Geological Survey Bulletin 1469, 40 p.

Steven, T.A., and Morris, H.T., 1983, Geologic map of the Cove Fort quadrangle, west-central Utah: U.S. Geological Survey Miscellaneous Investigations Series Map I-1481, scale 1:50,000.

Steven, T.A., and Morris, H.T., 1986, Summary mineral resource appraisal of the Richfield $1^\circ \times 2^\circ$ quadrangle, west-central Utah: U.S. Geological Survey Circular 916, 24 p.

Steven, T.A., Morris, H.T., and Rowley, P.D., 1990, Geologic map of the Richfield $1^\circ \times 2^\circ$ quadrangle, west-central Utah: U.S. Geological Survey Miscellaneous Investigations Series Map, I-1901, 3 maps on 1 sheet, scales 1:250,000 and 1:500,000.

Steven, T.A., Rowley, P.D., and Cunningham, C.G., 1984, Calderas of the Marysvale volcanic field, west-central Utah: Journal of Geophysical Research, v. 89, B10, p. 8751-8764.

Thompson, G.A., and Zoback, M.L., 1979, Regional geophysics of the Colorado Plateau: Tectonophysics, v. 61, p. 149-181.

Tweto, Ogden, and Case, J.E., 1972, Gravity and magnetic features as related to geology in the Leadville 30-minute quadrangle, Colorado: U.S. Geological Survey Professional Paper 726-C, 31 p. and 2 plates.

U.S. Department of Energy, 1982, Aerial radiometric and magnetic survey, Marysvale detail survey, Richfield national topographic map sheet, Utah: U.S. Department of Energy Open-File Report GJBX-37(78), 57 p.

Table 1. *Description and physical properties of igneous rock samples from the Marysvale volcanic field,Utah.*

[Map unit symbols explained in table 2. Abbreviations used in "Class" column explained in table 3. Susc., magnetic susceptibility; NRM, natural remanent magnetization; Q, Koenigsberger Q; ρ, dry bulk density, in g/cm^3. --, not applicable. Multiply values in the Susc. and NRM columns by $\times 10^{-3}$ to convert to cgs system and emu/cm^3, respectively.]

Sample No.	Map unit	Class	Latitude, longitude	Susc.	NRM	Q	ρ
M27A	Fresh quartz monzonite (Tbci), collected from the central intrusion near the Freedom Mine.	I-M	38°29'45" N., 112°12'47" W.	4.128	1.978	0.891	2.721
M30	Altered, dense, pink, alunitized Bullion Canyon Volcanics lava flow (Tbc), collected from the Whitehorse Mine.	M-BC	38°28'25" N., 112°11'27" W.	0.002	0.000187	0.178	2.366
M47B	Highly altered, alunitized Bullion Canyon Volcanics lava flow (Tbc), collected from the Yellow Jacket Mine.	H-BC	38°32'04" N., 112°12'30" W.	0.0008	0.00547	13.029	1.969
M49A	Devitrified, crystal-rich rhyolite intrusion (Tmi), collected from the Teacup dome.	I-R	38°30'41" N., 112°10'35" W.	0.790	0.366	0.858	2.319
M50	Fresh, fine-grained granite (Tmf), collected from the north end of the Central Mining Area.	I-G	38°30'24" N., 112°13'10" W.	0.684	0.231	0.625	2.520
M53	Highly altered, alunitized Bullion Canyon Volcanics lava flow (Tbc), collected from the Winkleman Mine.	H-BC	38°29'38" N., 112°17'32" W.	0.0004	0.00103	4.421	2.652
M75	Devitrified, crystal-rich tuff member of the Mount Belknap Volcanics (Tmc), collected along Beaver Creek, 1.45 km west of the junction of Beaver Creek and the Sevier River.	U-MB, X-TD	38°28'37" N., 112°14'57" W.	0.514	1.955	7.050	2.419
M88	Fresh Gray Hills Rhyolite Member of the Mount Belknap Volcanics (Tmg), collected 2.57 km west-northwest of the junction of Beaver Creek and the Sevier River.	U-MB, X-R	38°29'05" N., 112°15'35" W.	0.454	0.188	0.765	2.316
M91	Fresh, moderately welded Joe Lott Tuff Member of the Mount Belknap Volcanics (Tmj), collected from a road cut along Clear Creek, 3.14 km west of the junction of Clear Creek and the Sevier River.	U-MB, X-TM	38°34'50" N., 112°17'31" W.	0.0092	0.167	33.582	1.715
M94	Fresh, moderately welded Joe Lott Tuff Member of the Mount Belknap Volcanics (Tmj), collected from a road cut on U.S. Highway 89, on south side of rest area alongside Deer Creek.	U-MB, X-TM	38°30'08" N., 112°15'24" W.	0.191	0.207	3.212	2.204
M98	Fresh quartz monzonite (Tbci), collected on Tip Top, near the Sevier Mine.	I-M	38°29'20" N., 112°24'31" W.	2.666	20.188	14.021	2.651

Table 1. *Description and physical properties of igneous rock samples from the Marysvale volcanic field,Utah—Continued.*

Sample No.	Map unit	Class	Latitude, longitude	Susc.	NRM	Q	ρ
M109A	Highly altered Bullion Canyon Volcanics lava flow (Tbc), collected near Deer Flat.	H-BC	38°30'20" N., 112°17'18" W	-0.00019	0.00105	- -	2.312
M109B	Moderately altered Bullion Canyon Volcanics lava flow (Tbc), collected near Deer Flat.	M-BC	38°30'20" N., 112°17'18" W.	0.0055	0.00482	1.638	2.336
M109C	Slightly altered Bullion Canyon Volcanics lava flow (Tbc), collected near Deer Flat.	S-BC	38°30'20" N., 112°17'18" W.	0.0045	0.0246	10.105	2.321
M109D	Fresh Bullion Canyon Volcanics lava flow (Tbc), collected near Deer Flat.	U-BC, X-D	38°30'20" N., 112°17'18" W.	0.0255	0.885	64.246	2.398
M145A	Slightly altered, light-yellow, middle tuff member of the Mount Belknap Volcanics (Tmm), collected on Signal Peak in the Mount Belknap caldera.	S-MB	38°27'42" N., 112°23'58" W.	0.0185	0.0133	1.330	2.256
M145B	Densely welded, hard, red, middle tuff member of the Mount Belknap Volcanics (Tmm), collected on Signal Peak in the Mount Belknap caldera.	U-MB, X-TD	38°27'42" N., 112°23'58" W.	0.401	58.676	271.171	2.353
M177	Fresh quartz monzonite (Tbci), collected from Tip Top near the headwaters of Fish Creek.	I-M	38°29'19" N., 112°25'14" W.	3.194	1.689	0.979	2.707
M194	Highly altered middle tuff member of the Mount Belknap Volcanics (Tmm), collected along the road across the southeast margin of the Mount Belknap caldera.	H-MB	38°23'49" N., 112°24'09" W.	0.0018	0.00163	1.630	1.981
M206	Fresh Mount Baldy Rhyolite Member of the Mount Belknap Volcanics (Tmb), collected at the North Fork of North Creek in the Mount Belknap caldera.	U-MB, X-R	38°23'53" N., 112°29'24" W.	0.636	0.0809	0.236	2.530
M220	Fresh, massive Mount Baldy Rhyolite Member of the Mount Belknap Volcanics (Tmb), collected on Mount Baldy in the Mount Belknap caldera.	U-MB, X-R	38°24'11" N., 112°25'50" W.	0.266	0.213	1.483	2.470
M223	Moderately altered Mount Baldy Rhyolite Member of the Mount Belknap Volcanics (Tmb), collected on ridge going north from Mount Baldy, near the center of the Mount Belknap caldera.	M-MB	38°26'22" N., 112°27'03" W.	0.663	0.0591	0.165	2.223
M225	Slightly altered, bleached white Mount Baldy Rhyolite Member of the Mount Belknap Volcanics (Tmb), collected near Indian Creek, in the Mount Belknap caldera.	S-MB	38°25'16" N., 112°29'08" W.	0.0046	0.0145	5.800	2.323

Table 1. *Description and physical properties of igneous rock samples from the Marysvale volcanic field,Utah—Continued.*

Sample No.	Map unit	Class	Latitude, longitude	Susc.	NRM	Q	ρ
M238	Highly altered, zeolitic Red Hills Tuff Member of the Mount Belknap Volcanics (Tmr), collected northwest of Marysvale near the Beaver Creek stock.	H-MB	38°27'58" N., 112°14'44" W.	0.00079	0.00154	3.620	1.652
M251	Fresh rhyolite intrusive rock of the Mount Belknap Volcanics (Tmic), collected from the North Fork of North Creek stock in the Mount Belknap caldera.	I-R	38°23'56" N., 112°27'09" W	0.0628	0.0921	2.716	2.414
M261	Fresh middle Bullion Canyon Volcanics lava flow (Tbm), collected near the head of Bullion Canyon.	U-BC, X-D	38°23'51" N., 112°23'25" W.	0.0186	2.001	199.055	2.534
M263	Propylitized upper Bullion Canyon Volcanics lava flow (Tbu), collected near Delano Peak.	S-BC	38°22'52" N., 112°23'29" W.	0.352	3.790	19.922	2.501
M330	Fresh, dense, dark-colored rhyolite intrusion of Mount Belknap Volcanics (Tmic), containing potassium crystals as much as 2 cm long, collected underground at the U-Beva prospect.	I-R	38°22'58" N., 112°31'12" W.	2.899	0.490	0.313	2.640
M468	Propylitized Mount Dutton Formation pyroxene-hornblende lava flow (Td), collected on the north side of the entrance to Oak Springs Canyon.	OX-D	38°18'12" N., 112°13'48" W.	1.335	9.027	12.519	2.627
M470	Slightly oxidized Mount Dutton Formation basaltic andesite lava flow (Td), collected from the top of the highest hill south of the entrance to Oak Springs Canyon.	OX-B	38°18'02" N., 112°14'02" W.	1.822	12.795	13.003	2.795
M472	Fresh, devitrified Osiris Tuff (To), collected on the crest of the ridge between Big Flat and City Creek Peak.	OX-TD	38°18'22" N., 112°20'50" W.	0.469	2.526	9.972	2.313
M489	Moderately welded, crystal-rich tuff member of the Mount Belknap Volcanics (Tmc), collected near Three Creeks reservoir	U-MB, X-TM	38°18'17" N., 112°24'36" W.	0.215	0.966	8.320	1.500
M504	Moderately welded tuff of Lion Flat (Ttl), collected from switchback above the powerhouse on Utah Highway 153.	OX-TM	38°16'12" N., 112°29'12" W.	0.337	0.668	3.673	1.684
M505	Fresh, porphyritic Formation of Lousy Jim (Sigmund, 1979) lava flow (Tlj), collected at vent area along Utah Highway 153. Field test showed reversed magnetic polarity.	OX-D	38°16'45" N., 112°27'31" W.	0.306	0.145	0.879	2.408
M519	Fresh vent facies volcanic rocks of Little Table (Tlt), basaltic andesite collected south of the Central Mining Area.	OX-B	38°27'08" N., 112°11'55" W.	2.548	0.894	0.650	2.615

Table 1. *Description and physical properties of igneous rock samples from the Marysvale volcanic field,Utah—Continued.*

Sample No.	Map unit	Class	Latitude, longitude	Susc.	NRM	Q	ρ
M520	Fresh, pyroxene-plagioclase Bullion Canyon Volcanics lava flow (Tbc), collected south of the Central Mining Area.	U-BC, X-TD	38°27'04" N., 112°12'27" W.	1.349	1.747	2.399	2.580
M522	Fresh quartz monzonite of the Bullion Canyon Volcanics (Tbci), collected south of the Central Mining Area near the Dark Horse Mine.	I-M	38°28'17" N., 112°13'04" W.	1.554	5.850	6.970	2.578
M549	Devitrified, crystal-rich rhyolite intrusive rock of the Mount Belknap Volcanics (Tmi), collected from the Four Horsemen dome.	I-R	38°29'52" N., 112°10'37" W.	0.442	1.118	4.680	2.291
M563	Altered, intermediate composition Bullion Canyon Volcanics lava flow (Tbc), collected near the Central Mining Area.	M-BC	38°28'21" N., 112°26'03" W.	0.00038	0.0109	53.107	1.956
M569	Fresh, coarse-grained monzonite from an intrusion related to the Monroe Peak caldera (Tmpi), collected from Dry Canyon, in the Monroe Peak caldera.	I-M	38°31'58" N., 112°07'35" W.	1.671	0.149	0.165	2.558
M575	Highly altered, bleached, iron-stained Blue Lake Rhyolite Member of the Mount Belknap Volcanics (Tmbl), collected near the Pipe- line Trail on Gold Mountain, in the Mount Belknap caldera.	H-MB	38°26'17" N., 112°23'55" W.	-0.00121	0.00258	- -	2.488
M581	Fresh, fine-grained lava flow of the Mount Baldy Rhyolite Member of the Mount Belknap Volcanics (Tmb), collected from the summit of Mount Belknap in the Mount Belknap caldera.	U-MB, X-R	38°25'10" N., 112°24'40" W.	0.288	2.586	16.635	2.492
M582	Moderately fresh middle tuff member of the Mount Belknap Volcanics (Tmm), collected near the summit of Mount Belknap in the Mount Belknap caldera.	U-MB, X-TD	38°25'10" N., 112°24'27" W.	0.151	0.140	1.707	2.306
M583	Moderately fresh Blue Lake Rhyolite Member of the Mount Belknap Volcanics lava flow (Tmbl), collected west of Mount Belknap in the Mount Belknap caldera.	U-MB, X-R	38°24'50" N., 112°23'45" W.	0.0030	0.000731	0.448	2.327
M584	Moderately fresh Mount Baldy Rhyolite Member of the Mount Belknap Volcanics lava flow (Tmb), collected west of Mount Belknap in the Mount Belknap caldera.	U-MB, X-R	38°24'03" N., 112°24'12" W.	0.0156	0.224	26.555	2.325
M586	Highly altered middle tuff member of the Mount Belknap Volcanics (Tmm), collected along the road across the southeast margin of the Mount Belknap caldera.	H-MB	38°23'50" N., 112°24'12" W.	0.0015	0.00131	1.656	2.004

Table 1. *Description and physical properties of igneous rock samples from the Marysvale volcanic field,Utah—Continued.*

Sample No.	Map unit	Class	Latitude, longitude	Susc.	NRM	Q	ρ
M608	Fresh quartz monzonite of the Bullion Canyon Volcanics (Tbci), collected from the stockunder the power line southeast of the Central Intrusion.	U-BC, I-M	38°29'05" N., 112°10'40" W.	1.318	0.392	0.550	2.518
M621	Fresh quartz monzonite of the Bullion Canyon Volcanics (Tbci), collected from the west side of Flattop in the Central Intrusion.	U-BC, I-M	38°30'23" N., 112°11'55" W.	5.682	3.432	1.118	2.731
M657	Fresh, potassium-rich mafic lava flows(Tpm), collected from Big Flat.	OX-B	38°16'16" N., 112°22'04" W.	2.946	2.322	1.495	2.621
M678	Fresh, sanidine-bearing dacitic lava flows (Tsd), collected above Hunt's lake on Monroe Peak.	OX-D	38°32'52" N., 112°05'04" W.	0.149	1.103	13.719	2.280
M713A	Highly altered Bullion Canyon Volcanics lava flow (Tbc), collected west of the La Veta Mine.	H-BC	38°31'22" N., 112°11'16" W	0.0116	0.000134	0.021	1.763
M713B	Highly altered Bullion Canyon Volcanics lava flow (Tbc), collected west of the La Veta Mine.	H-BC	38°31'22" N., 112°11'16" W.	0.0042	0.00235	1.024	1.617
M739	Fresh mafic tuff of Albinus Canyon (Tal), collected from the type area near Albinus Canyon in the Pavant Range.	OX-TD	38°41'17" N., 112°11'09" W.	1.516	0.190	0.232	2.600
M755	Fresh fine-grained monzonite from an intrusion related to the Monroe Peak caldera (Tmpi),collected from the west side of the Sevier Plateau, north of Dry Canyon.	I-M	38°32'34" N., 112°07'51" W.	0.0119	0.0260	4.038	2.499
M798	Fresh, potassium-rich mafic lava flow (Tpm), collected northeast of Junction, near the Piute Reservoir.	OX-B	38°15'12" N., 112°12'43" W.	1.967	16.015	15.073	2.642
M800	Fresh basalt (Tbas), collected from the ridge east of Piute Reservoir.	OX-B	38°18'50" N., 112°09'22" W.	2.795	13.133	8.702	2.597
M801	Fresh basalt (Tbas), collected from hill north of City Creek.	OX-B	38°15'48" N., 112°17'16" W.	1.750	26.083	27.601	2.655
M809	Poorly welded Joe Lott Tuff Member of the Mount Belknap Volcanics (Tmj), collected from the distal end of the ash sheet, near Monroe.	U-MB, X-TP	38°34'18" N., 112°08'10" W.	0.0123	0.321	48.381	1.795
M824	Fresh, potassium-rich mafic lava flow (Tpm), collected on Black Ridge, east of Beaver.	OX-B	38°18'08" N., 112°33'24" W.	1.613	17.062	19.951	2.788

Table 1. *Description and physical properties of igneous rock samples from the Marysvale volcanic field,Utah—Continued.*

Sample No.	Map unit	Class	Latitude, longitude	Susc.	NRM	Q	ρ
M851	Fresh quartz monzonite intrusion of theBullion Canyon Volcanics (Tbci), collected from the Central Intrusion just west of the Royal Purple Mine.	U-BC, I-M	38°30'43" N., 112°13'05" W.	3.816	53.486	25.955	2.736
M859	Fresh, densely welded, red middle tuff Member of the Mount Belknap Volcanics(Tmm), collected from the Hogback in the Mount Belknap caldera.	U-MB, X-TD	38°29'05" N., 112°27'05" W.	0.802	11.076	25.560	2.332
M864	Slightly altered, pyrite-bearing lava flow of the Blue Lake Rhyolite Member of the Mount BelknapVolcanics (Tmbl), collected from altered area east of Blue Lake.	S-MB	38°24'37" N., 112°24'53" W.	0.00283	0.00117	0.767	2.412
M867	Fresh quartz monzonite intrusion of theBullion Canyon Volcanics (Tbci), collected from the Central Intrusion at the north end of the Central Mining Area.	U-BC, I-M	38°30'19" N., 112°12'52" W.	3.403	1.131	0.616	2.732
M873	Highly altered, alunitized Bullion Canyon Volcanics lava flow (Tbc), collected from the upper pit of the Whitehorse Mine.	H-BC	38°28'24" N., 112°11'23" W.	-0.00224	0.000977	- -	2.162
M874	Highly altered, kaolinitized Joe Lott Tuff Member of the Mount Belknap Volcanics (Tmj), collected from the Mill Creek kaolinite pit.	H-MB	38°31'14" N., 112°23'21" W.	-0.00049	0.0232	- -	2.032
M881	Highly altered, white, alunitized Bullion Canyon Volcanics lava flow (Tbc), collectedfrom the south end of Big Rock Candy Mountain.	H-BC	38°30'20" N., 112°15'41" W.	-0.00246	0.00190	- -	1.910
M883	Moderately altered, pyrite-bearing Bullion Canyon Volcanics lava flow (Tbc), collected from Big Rock Candy Mountain.	M-BC	38°30'38" N., 112°15'43" W.	0.00147	0.00107	1.355	2.387
M885	Highly altered, yellow lava flow of the Bullion Canyon Volcanics (Tbc), collected behind the Big Rock Candy Mountain resort.	H-BC	38°30'52" N., 112°15'56" W.	0.00485	0.00565	2.155	2.232
M902	Fresh Delano Peak Tuff Member of the Bullion Canyon Volcanics (Tbcd), collected near the summit of the Tushar Mountains, north of Delano Peak.	U-BC, X-TD	38°23'22" N., 112°23'50" W.	0.191	0.125	1.207	2.323
M903	Fresh mafic lava flow in the upper Bullion Canyon Volcanics (Tbu), collected in the Big John caldera.	U-BC, X-D	38°23'09" N., 112°23'50" W.	0.815	76.729	174.428	2.591
M905	Fresh mafic lava flow in the upper Bullion Canyon Volcanics (Tbu), collected from the same flow that caps Delano Peak. Field test showed normal magnetic polarity.	U-BC, X-B	38°22'05" N., 112°23'27" W.	0.656	0.732	2.067	2.531

Table 1. *Description and physical properties of igneous rock samples from the Marysvale volcanic field,Utah—Continued.*

Sample No.	Map unit	Class	Latitude, longitude	Susc.	NRM	Q	ρ
M907	Fresh, densely welded Three Creeks Tuff Member of the Bullion Canyon Volcanics(Tbct), collected from the Narrows along Utah Highway 4.	U-BC, X-TD	38°34'51" N., 112°07'36" W.	0.741	0.759	1.897	2.533
M908	Fresh, moderately welded Three Creeks Tuff Member of the Bullion Canyon Volcanics(Tbct), collected from the Narrows along Utah Highway 4. Field test showed normal magnetic polarity.	U-BC, X-TM	38°34'52" N., 112°07'45" W.	0.364	1.065	5.418	2.386
M910	Fresh basaltic andesite lava flow (Tan) collected along the Rockwood Station road in the Pavant Range. Field test showed normal magnetic polarity.,	OX-B	38°38'26" N., 112°16'12" W.	1.448	8.111	10.376	2.447
M912	Fresh, densely welded tuff from the lower part of the Three Creeks Tuff Member of the Bullion Canyon Volcanics (Tbct). Collected near the Joseph Hot Spring.	U-BC, X-TD.	38°37'31" N., 112°11'35" W.	0.163	0.378	4.284	2.191
M913	Fresh, densely welded tuff of Albinus Canyon (Tal), collected near the JosephHot Spring.	OX-TD	38°37'30" N., 112°11'25" W.	0.290	0.294	1.879	1.975
M914	Fresh, medium-grained monzonite forming one of the intrusions related to the Monroe Peak caldera (Tmpi), collected from Flat Canyon on the west side of the Sevier Plateau.	I-M	38°29'02" N., 112°07'30" W.	0.851	0.230	0.501	2.487
M915	Fresh, medium-grained monzonite forming one of the intrusions related to the Monroe Peak caldera (Tmpi), collected from Smith Canyon, on the west side of the Sevier Plateau.	I-M	38°27'31" N., 112°06'33" W.	0.723	0.277	0.709	2.520
M928	Moderately welded tuff of Lion Flat (Ttl), collected on ridge south of South Fork ofNorth Creek, probably in the source area.	OX-TM	38°19'34" N., 112°32'00" W.	0.160	1.030	11.933	1.849
M929	Propylitized mafic pyroxene-plagioclase lava flow in Bullion Canyon Volcanics (Tbc), collected along Pine Creek, in the western Tushar Mountains.	S-BC	38°30'07" N., 112°33'07" W.	1.251	0.111	0.164	2.349
M930A	Fresh, porphyritic monzonite intrusion of the Bullion Canyon Volcanics (Tbci), collected along Pine Creek in the Western Tushar Mountains.	U-BC, I-M	38°29'48" N., 112°32'50" W.	0.514	0.609	2.195	2.303

Table 1. *Description and physical properties of igneous rock samples from the Marysvale volcanic field,Utah—Continued.*

Sample No.	Map unit	Class	Latitude, longitude	Susc.	NRM	Q	ρ
M930D	Fresh, porphyritic monzonite intrusion of the Bullion Canyon Volcanics (Tbci), collectedalong Pine Creek in the Western Tushar Mountains.	U-BC, I-M	38°29'48" N., 112°32'50" W.	0.463	0.538	2.149	2.466
75-S-20	Propylitized Three Creeks Tuff Member of the Bullion Canyon Volcanics (Tbct), collected on the south side of Bullion Canyon, 1.84 km northeast of Mount Brigham.	S-BC	38°23'23" N., 112°20'00" W.	0.0161	0.141	16.209	2.587
79-S-44B	Fresh, slightly vesicular, basaltic andesite lava flow (Qb), collected about 13 kmwest of Cove Fort, on the western flank of the Cove Fort shield volcano.	OX-B	38°35'23" N., 112°43'35" W.	1.469	62.768	79.111	2.602
78-698	Fresh flow breccia from alluvial facies of Mount Dutton Formation (Td), collected east of Piute Reservoir, central Sevier Plateau.	OX-B	38°16'12" N., 112°10'30" W.	4.623	6.061	2.427	2.594
79-1517	Fresh dacitic lava flow from vent faciesvolcanics of Langdon Mountain (Tlm), collected from the central Sevier Plateau.	OX-D	38°23'50" N., 112°01'50" W.	2.561	3.002	2.171	2.709
79-1518	Fresh lava flow from vent facies of volcanics of Little Table (Tlt). Dacitic andesite, more mafic than sample 79-1517.	OX-B	38°22'20" N., 112°04'58" W.	2.467	0.704	0.528	2.606
79-1666	Fresh lava flow from vent facies of Bullion Canyon Volcanics (Tbc), collected in Monroe Canyon, southeast of Monroe, in the northern Sevier Plateau.	U-BC, X-B	38°35'57" N., 112°05'05" W.	2.304	0.153	0.123	2.647

Table 2. *Description of map units for the Marysvale volcanic field, Utah.*

amygdaloidal flows. Some of these flows are inferred to have reversed magnetic polarity

Tlj **Formation of Lousy Jim (Sigmund, 1979) (Miocene)**—Light- to dark-gray, quartz latitic porphyry lava flows and flow breccia. Contains 23 percent phenocrysts of plagioclase, amphibole, clinopyroxene, magnetite, biotite, quartz, and accessory minerals in a glassy groundmass

Ttl **Tuff of Lion Flat (Miocene)**—Light-gray to grayish-pink, ash-flow tuff consisting of glass shards, pumice fragments, and volcanic dust, and about 5-15 percent phenocrysts of plagioclase, quartz, sanidine, biotite, and amphibole. Locally reworked and zeolitized

Tsd **Sanidine-bearing dacitic lava flows (Miocene)**—Resistant to moderately resistant, generally light- to dark-gray and dark-brown, locally vesicular or amygdaloidal, locally flow layered dacitic lava flows. Locally includes volcanic mudflow breccia and ash-flow tuff. Contains moderately abundant phenocrysts of plagioclase, sanidine, pyroxene, and biotite, and minor Fe-Ti oxides and olivine; sanidine phenocrysts may be as long as 2 cm. Considered to be the extrusive equivalent of the resurgent intrusive rocks (Tmpi) that invaded the volcanic rocks filling the Monroe Peak caldera

Tmpi **Intrusions related to the Monroe Peak Caldera (Miocene)**—Generally resistant, light-gray and grayish-green monzonite porphyry and subordinate quartz monzonite porphyry. Constitutes the main resurgent phase of the intrusions related to the Monroe Peak caldera. Contains large phenocrysts of plagioclase and orthoclase, with smaller pyroxene and biotite, in a groundmass dominated by orthoclase, Fe-Ti oxides, and quartz. A fine-grained, more potassic phase is present in the upper parts of some intrusions

To **Osiris Tuff (Miocene)**—Gray and reddish-brown, densely welded, crystal-rich ash-flow tuff. Phenocrysts consist of andesine and subordinate sanidine, pyroxene, and minor biotite, and Fe-Ti oxides

Bullion Canyon Volcanics (Miocene and Oligocene)

Tbci **Intermediate-composition intrusive rock (Miocene)**—Dark- to light-gray and brown, strongly porphyritic quartz latite and latite and porphyritic to equigranular, fine- to medium-grained quartz monzonite, monzonite, and granodiorite. The more crystalline rocks commonly contain approximately equal proportions of plagioclase and orthoclase, 0-20 percent quartz, plus augite, hornblende, and biotite. Accessory minerals are apatite, zircon, and Fe-Ti oxides

Tbu **Upper member (Miocene)**—Mostly dark-gray to black, fine-grained rhyodacite to andesite lava flows and local densely welded ash-flow tuff, some of which show prominent lineate texture due to secondary flowage. Overlies Delano Peak Tuff Member in central Tushar Mountains

Tbcd **Delano Peak Tuff Member (Miocene)**—Dark-reddish-brown, densely welded, crystal-rich quartz latite ash-flow tuff containing 40-50 percent phenocrysts of andesine, hornblende, biotite, and minor quartz, zircon, and apatite. Source area is Big John caldera, in central Tushar Mountains

Tbm **Middle member (Miocene and Oligocene)**—Mostly light-gray and brown rhyodacite lava flows, flow breccia, and volcanic mudflow breccia that lie between the overlying Delano Peak Tuff Member (Tbcd) and underlying Three Creeks Tuff Member (Tbct) in the central Tushar Mountains

Table 2. *Description of map units for the Marysvale volcanic field, Utah.*

Tbct **Three Creeks Tuff Member (Oligocene)**—Light-gray and brown, densely welded, crystal-rich quartz latite ash-flow tuff containing 45-50 percent phenocrysts of plagioclase, hornblende, biotite, and quartz, with trace amounts of Fe-Ti oxide minerals, sanidine, and other accessory minerals

Tbc **Heterogeneous lava flows and volcanic breccia (Miocene and Oligocene)**—Porphyritic andesite, rhyodacite, and quartz latite. Contains phenocrysts of plagioclase, biotite, and clinopyroxene. In part consists of fine-grained, dark lava flows and breccia of intermediate composition, containing small phenocrysts of plagioclase and clinopyroxene

Tal **Tuff of Albinus Canyon (Miocene or Oligocene)**—Red to gray, vesicular, densely welded ash-flow tuff (tufflava) containing a few percent phenocrysts of calcic andesite-labradorite, augite, and biotite in a glassy to devitrified matrix. Prominent fluidal textures from secondary flow and very abundant lineate vesicles are characteristic

Ta **Basaltic andesite (Miocene or Oligocene)**—Vesicular, black to dark-gray lava flows containing phenocrysts of calcic labradorite, pyroxene, magnetite, and olivine (altered to iddingsite) in a glassy to microgranular matrix

Tlm **Vent facies volcanic rocks of Langdon Mountain (Miocene)**—Resistant, pink, tan, light-gray, purplish- gray, locally amygdaloidal lava flows of dacitic composition that overlie, and are interbedded with, the upper part of both the Mount Dutton Formation (Td) and the volcanic rocks of Little Table (Tlt). The rocks are part of a stratovolcano centered at or near Langdon Mountain. Contain phenocrysts of hornblende, subordinate plagioclase and pyroxene, and minor Fe-Ti oxides

Tlt **Vent facies volcanic rocks of Little Table (Miocene and Oligocene)**--Resistant, tan, khaki, dark-gray to dark-brown lava flows, tuff lava, flow breccia, and volcanic mudflow breccia that are interbedded with, pinch out southward against, and locally underlie the Mount Dutton Formation and are interbedded with and underlie the lower parts of the volcanic rocks of Langdon Mountain. Contains phenocrysts of plagioclase and generally subordinate pyroxene and Fe-Ti oxides and minor olivine

Td **Mount Dutton Formation (Miocene and Oligocene)**—Soft to moderately resistant, tan, pink, light-gray, or less commonly pale-green or light-purple volcanic mudflow breccia and sparse flow breccia, lava flows, local ash-flow tuff, and fluviatile conglomerate and sandstone. Flow rock and clasts in the breccia are characterized by several lithologies that are dacitic to andesitic in composition and have few phenocrysts; many rocks are aphanitic. Phenocrysts consist largely of plagioclase and either hornblende or pyroxene and minor Fe-Ti oxides. Inferred to contain subunits having reverse magnetic polarity

Tn **Needles Range Group (Oligocene)**—Gray, tan, or pink, moderately welded quartz latite ash-flow tuff consisting of 40-50 percent phenocrysts of andesine, hornblende (10-15 percent), biotite, and minor sanidine, quartz, pyroxene, and Fe-Ti oxides. The high hornblende-to-biotite ratio is a distinguishing characteristic. Rocks regionally mapped as unit Tn in the Pavant Range and adjacent area (Cunningham and others, 1983) have been shown (Myron Best, written commun., 1985) to be lower units in the Three Creeks Tuff Member of the Bullion Canyon Volcanics. Inferred to contain subunits having reversed magnetic polarity

Table 3. *Abbreviations used in this report to indicate sample classes.*

First classification type: lithology	Second classification type: degree of alteration
X, OX Extrusive rocks -R Rhyolites -D Dacites -B Basaltic rocks -TP Tuff, poorly welded -TM Tuff, moderately welded -TD Tuff, densely welded I Intrusive rocks -R Intrusive rhyolites -G Granitic rocks -M Monzonites	U Unaltered S Slightly altered (propylitic alteration) M Moderately altered (argillic alteration) H Highly altered (advanced argillic alteration) -BC Bullion Canyon Volcanics rocks -MB Mount Belknap Volcanics rocks -OX Other extrusive rocks, neither BC nor MB

Table 4. *Summary of properties found for duplicate samples*.

[DBD, dry bulk density, in g/cm^3 ; Susc., magnetic susceptibility, in cgs system; NRM, natural remanent magnetization, in emu/cm^3 ; Q, Koenigsberger ratio. E denotes exponent; that is, 1.97E-03 =1.97×10^{-3}. Class designations are explained in table 3.]

Sample	Class	DBD	Mass	Susc.	NRM	Q
M798	OX-B	2.642	2.36	1.97E-03	1.60E-02	15.073
		2.642	2.04	1.94E-03	8.15E-03	7.793
M859	U-MB,	2.332	2.20	7.90E-04	1.03E-02	24.163
	X-TD	2.332	1.45	8.02E-04	1.11E-02	25.560
M930D	U-BC,	2.466	2.38	4.62E-04	5.09E-04	2.039
	I-M	2.466	2.28	4.63E-04	5.38E-04	2.149
79-1517	OX-D	2.709	2.23	2.56E-03	3.00E-03	2.171
		2.709	2.19	2.59E-03	2.22E-03	1.589
79-1518	OX-B	2.606	1.71	2.40E-03	6.50E-04	0.501
		2.606	1.37	2.47E-03	7.04E-04	0.528

Table 5(a). *Statistics of density measurements of rock samples from Marysvale volcanic field, Utah.*

[N, number of samples in class; Min, minimum value measured for that class; m, sample mean; SD, standard deviation of the sample; SE, standard error of the sample; Max, maximum value measured for that class; --, not applicable. Class designations are explained in table 3.]

Class	N	Min	m-SD	m-SE	mean, m	m+SE	m+SD	Max
H-MB	5	1.652	1.733	1.898	2.031	2.165	2.330	2.488
H-BC	9	1.617	1.785	2.001	2.109	2.217	2.433	2.652
M-MB	1	--	--	--	2.223	--	--	--
M-BC	3	1.959	1.994	2.092	2.227	2.362	2.461	2.387
S-MB	3	2.256	2.252	2.285	2.330	2.376	2.409	2.412
S-BC	4	2.321	2.313	2.376	2.440	2.503	2.566	2.587
U-MB	14	1.500	1.905	2.136	2.220	2.305	2.536	2.530
U-BC	10	2.191	2.329	2.426	2.471	2.516	2.613	2.647
I-R	4	2.291	2.258	2.337	2.416	2.495	2.574	2.640
I-G	1	--	--	--	2.520	--	--	--
I-M	14	2.303	2.455	2.551	2.586	2.621	2.717	2.736
X-TP	1	--	--	--	1.795	--	--	--
X-TM	6	1.500	1.552	1.752	1.890	2.028	2.228	2.386
X-TD	11	1.975	2.177	2.303	2.357	2.411	2.537	2.600
X-R	6	2.316	2.312	2.370	2.410	2.450	2.508	2.530
X-D	7	2.280	2.356	2.450	2.507	2.564	2.657	2.709
X-B	13	2.447	2.535	2.601	2.626	2.652	2.718	2.795

Table 5(b). *Statistics of susceptibility measurements of rock samples from Marysvale volcanic field, Utah.*

Class	N	Min	m-SD	m-SE	mean, m	m+SE	m+SD	Max
H-MB	3	7.89E-7	8.29E-7	1.06E-6	1.29E-6	1.57E-6	2.00E-6	1.85E-6
H-BC	6	4.33E-7	6.80E-7	1.54E-6	2.32E-6	3.50E-6	7.94E-6	1.16E-5
M-MB	1	--	--	--	6.63E-4	--	--	--
M-BC	3	3.79E-7	3.82E-7	6.70E-7	1.45E-6	3.12E-6	5.48E-6	5.45E-6
S-MB	3	2.83E-6	2.36E-6	3.55E-6	6.23E-6	1.09E-5	1.65E-5	1.85E-5
S-BC	4	4.50E-6	5.48E-6	2.03E-5	7.52E-5	2.79E-4	1.03E-3	1.25E-3
U-MB	11	3.02E-6	1.87E-5	7.10E-5	1.16E-4	1.88E-4	7.12E-4	8.02E-4
U-BC	10	1.86E-5	6.08E-5	1.83E-4	3.04E-4	5.05E-4	1.51E-3	2.30E-3
I-R	4	6.28E-5	1.02E-4	2.26E-4	5.02E-4	1.11E-3	2.47E-3	2.90E-3
I-G	1	--	--	--	6.84E-4	--	--	--
I-M	14	1.19E-5	2.57E-4	8.03E-4	1.22E-3	1.84E-3	5.75E-3	5.68E-3
X-TP	1	--	--	--	1.23E-5	--	--	--
X-TM	6	9.20E-6	3.30E-5	7.40E-5	1.29E-4	2.25E-4	5.04E-4	3.64E-4
X-TD	11	1.51E-4	2.03E-4	3.55E-4	4.52E-4	5.76E-4	1.01E-3	1.52E-3
X-R	6	3.02E-6	1.15E-5	4.16E-5	1.01E-4	2.44E-4	8.79E-4	6.36E-4
X-D	7	1.86E-5	3.70E-5	1.21E-4	2.50E-4	5.14E-4	1.68E-3	2.56E-3
X-B	13	6.56E-4	1.25E-3	1.75E-3	1.99E-3	2.27E-3	3.17E-3	4.62E-3

Table 5(c). *Statistics of natural remanent magnetization measurements of rock samples from Marysvale volcanic field, Utah*.

Class	N	Min	m-SD	m-SE	mean, m	m+SE	m+SD	Max
H-MB	5	1.31E-6	8.71E-7	1.69E-6	2.88E-6	4.91E-6	9.50E-6	2.32E-5
H-BC	9	1.34E-7	3.13E-7	7.47E-7	1.16E-6	1.79E-6	4.27E-6	5.65E-6
M-MB	1	--	--	--	5.91E-5	--	--	--
M-BC	3	1.07E-6	1.18E-6	1.94E-6	3.83E-6	7.55E-6	1.24E-5	1.09E-5
S-MB	3	1.17E-6	1.46E-6	2.67E-6	6.08E-6	1.39E-5	2.53E-5	1.45E-5
S-BC	4	2.46E-5	2.34E-5	6.76E-5	1.95E-4	5.65E-4	1.63E-3	3.79E-3
U-MB	14	7.31E-7	2.93E-5	1.99E-4	3.99E-4	8.02E-4	5.43E-3	5.87E-2
U-BC	10	1.25E-4	1.68E-4	5.69E-4	1.00E-3	1.76E-3	5.96E-3	7.67E-2
I-R	4	9.21E-5	1.31E-4	2.19E-4	3.69E-4	6.20E-4	1.04E-3	1.12E-3
1-G	1	--	--	--	2.31E-4	--	--	--
1-M	14	2.60E-5	1.44E-4	6.26E-4	1.07E-3	1.83E-3	7.98E-3	5.35E-2
X-TP	1	--	--	--	3.21E-4	--	--	--
X-TM	6	1.67E-4	2.31E-4	3.81E-4	5.39E-4	7.60E-4	1.25E-3	1.07E-3
X-TD	11	1.25E-4	1.50E-4	5.81E-4	1.04E-3	1.87E-3	7.21E-3	5.87E-2
X-R	6	7.31E-7	7.09E-6	3.50E-5	1.05E-4	3.17E-4	1.57E-3	2.59E-3
X-D	7	1.45E-4	3.47E-4	1.18E-3	2.49E-3	5.24E-3	1.79E-3	7.67E-2
X-B	13	1.53E-4	8.13E-4	2.91E-3	4.74E-3	7.72E-3	2.46E-2	6.28E-2

Table 5(d). *Statistics of Konigsberger Q measurements of rock samples from Marysvale volcanic field, Utah.*

Class	N	Min	m-SD	m-SE	mean, m	m+SE	m+SD	Max
H-MB	3	1.630	1.355	1.743	2.138	2.622	3.373	3.620
H-BC	6	0.021	0.086	0.408	0.885	1.924	9.079	13.029
M-MB	1	--	--	--	0.165	--	--	--
M-BC	3	1.355	0.621	1.488	4.903	16.156	38.678	53.107
S-MB	3	0.767	0.635	1.072	1.808	3.051	5.148	5.800
S-BC	4	0.164	0.497	1.547	4.811	14.965	46.548	19.922
U-MB	14	0.236	0.855	3.735	6.396	10.952	47.853	271.171
U-BC	10	0.123	0.574	2.891	6.108	12.904	65.031	199.053
I-R	4	0.313	0.406	0.743	1.359	2.487	4.549	4.680
I-G	1	--	--	--	0.625	--	--	--
I-M	14	0.165	0.401	1.120	1.630	2.372	6.635	25.955
X-TP	1	--	--	--	48.381	--	--	--
X-TM	6	3.212	3.231	5.414	7.729	11.034	18.486	33.581
X-TD	11	0.232	0.675	2.447	4.267	7.439	26.965	271.169
X-R	6	0.236	0.276	0.871	1.938	4.294	13.606	26.554
X-D	7	0.879	2.271	8.362	18.462	40.760	150.069	199.053
X-B	13	0.123	0.694	2.638	4.403	7.349	27.919	79.110

Table 6. *Typical values of physical properties for rocks of the Marysvale volcanic field, Utah.*

Rock type	Density (g/cm^3)	Susceptibility ($\times 10^{-4}$ cgs)	NRM ($\times 10^{-4}$ emu)
Mount Belknap Volcanics extrusive rocks			
Highly altered	2.0	0.01	0.03
Moderately altered	2.2	0.04	0.04
Slightly altered	2.3	0.06	0.06
Unaltered	2.3	1.0	4.0
Bullion Canyon Volcanics extrusive rocks			
Highly altered	2.0	0.02	0.01
Moderately altered	2.2	0.02	0.04
Slightly altered	2.4	0.8	2.0
Unaltered	2.5	3.0	10.0
Intrusive rocks			
Intrusive rhyolites	2.4	5.0	4.0
Granites	2.5	7.0	6.0
Monzonites	2.6	12.0	10.0
Tuffs			
Poorly welded	1.8	0.2	3.0
Moderately welded	1.9	2.0	6.0
Densely welded	2.3	5.0	10.0
Extrusive rocks			
Extrusive rhyolites	2.4	1.0	1.0
Intermediate composition rocks	2.5	2.5	25.0
Mafic composition rocks	2.6	20.0	45.0

INDEX TO GEOPHYSICAL FEATURES DISCUSSED